

From the Department of Clinical Science, Intervention and
Technology, Division of Renal Medicine,
Karolinska Institutet, Stockholm, Sweden

**THE EXPRESSION OF THE
STRUCTURAL PROTEINS
DENDRIN, PLEKHH2 AND
NEPH1 IN THE
GLOMERULAR FILTRATION
BARRIER**

Jenny Hulkko



**Karolinska
Institutet**

Stockholm 2015

All previously published papers were reproduced with permission from the publisher.

Published by Karolinska Institutet. Printed by E-Print AB.

© Jenny Hulkko, 2015
ISBN 978-91-7549-944-4

TO MIKAEL AND JULIUS

From the Department of Clinical Science, Intervention and Technology, Division of
Renal Medicine

The expression of the structural proteins Dendrin, Plekhh2 and Neph1 in the glomerular filtration barrier

Akademisk avhandling

Som för avläggande av doktorsexamen vid Karolinska Institutet
offentligen försvaras i föreläsningssal 4V, Odontologhuset, plan
4, Alfred Nobels Allé 8, Huddinge.

Fredagen den 22 maj, 2015, klockan 10.00

av

Jenny Hulkko

Huvudhandledare:

Docent Annika Wernerson
Karolinska Institutet
Institutionen för Klinisk Vetenskap,
Intervention och Teknik,
Enheten för Medicinska Njursjukdomar

Opponent:

Docent Johan Mölne
Göteborgs Universitet
Institutionen för Biomedicin,
Avdelningen för Patologi

Bihandledare:

Docent Kjell Hultenby
Karolinska Institutet
Institutionen för Laboratoriemedicin,
Avdelningen Kliniskt Forskningscentrum

Betygsnämnd:

Med. Dr Inga Soveri
Uppsala Universitet
Institutionen för Medicinska Vetenskaper,
Avdelningen för Njurmedicin

Med. Dr Fredrik Dunér
Karolinska Institutet
Institutionen för Klinisk Vetenskap,
Intervention och Teknik,
Enheten för Medicinska Njursjukdomar

Docent Alexei Terman
Karolinska Institutet
Institutionen för Laboratoriemedicin,
Avdelningen för Patologi

Med. Dr Jaakko Patrakka
Karolinska Institutet
Institutionen för Medicin,
Integrated CardioMetabolic Center

Professor Bengt Fellström
Uppsala Universitet
Institutionen för Medicinska Vetenskaper,
Avdelningen för Njurmedicin

ABSTRACT

Background

The podocytes are injured in many acquired glomerular diseases. This may present as proteinuria or morphological changes such as foot process effacement (FPE) or loss of podocytes in the urine. The exact mechanisms are still mainly unknown. However, a number of proteins identified in the slit diaphragm (SD) of the podocytes, including Dendrin and Neph1, are believed to be of significance in the podocytes' response to injury and in the resulting pathophysiological development. Dendrin was primarily found to be associated to the actin cytoskeleton in mouse podocytes. Neph1 is a transmembrane protein that together with Neph1rin forms a complex in the SD, involved in polymerization of the actin cytoskeleton and proteinuria. Plekhh2 is an uncharacterized protein that we localized to the podocyte cytoplasm.

Aim

The principal aim was to study the expression and role of novel structural glomerular proteins in acquired human glomerular disease. In the first study, focusing on the expression of Dendrin in normal human kidney and in the glomerular disease Minimal Change Nephrotic Syndrome (MCNS), light and immune electron microscopy (iEM) was used. In the second study, the subcellular localization of the uncharacterized protein Plekhh2 in normal human kidney and Focal Segmental Glomerulosclerosis (FSGS) was investigated by immunofluorescence (IFL) and iEM. Neph1 and Neph1rin were studied in FSGS, MCNS and in the corresponding experimental models Adriamycin nephropathy (ADR) and puromycin aminonucleoside nephrosis (PAN). Lastly, we returned to Dendrin, and studied the expression in the podocyte nuclei in IgA Nephropathy (IgAN) and Membranous Nephropathy (MN) with iEM and analyzed the gene expression with microarray.

Results

Dendrin was localized to the glomerular slit diaphragm (SD). There was no significant change in the amount of Dendrin in MCNS compared to controls by IFL and iEM. In areas of FPE Dendrin was redistributed from the SD to the podocyte cytoplasm. Plekhh2 was localized mainly to the podocyte cytoplasm. The expression was reduced in FSGS. Double staining of Neph-1 and Neph1rin showed the proteins in close connection in the SD. Neph1 was significantly reduced in FSGS, MCNS, ADR and PAN. The reduction of Neph1 was also seen in areas without FPE. Neph1rin was unchanged in FSGS, but reduced in MCNS and PAN. Dendrin was increased in the podocyte nuclei in IgAN, with a corresponding two fold increase of the gene expression. Both protein and gene expression of Dendrin was unchanged in MN.

Conclusion

In preserved slits and in areas without FPE in MCNS, the amounts of Dendrin were unchanged compared to controls. The redistribution might therefore be secondary to FPE, *per se*. However, the increase of nuclear Dendrin in IgAN suggests an upregulated apoptotic pathway and a possible role for Dendrin in the pathogenesis of this disease. Plekhh2 was reduced and relocated from the plasma membrane to centrally in the foot processes in FSGS. Neph1 was reduced in FSGS, MCNS, ADR and PAN, in contrast to Neph1rin which was unchanged in FSGS. This could indicate a disruption of the Neph1-Neph1rin complex and an involvement of Neph1 in the pathogenesis of this disease.

1 LIST OF PUBLICATIONS

- I) Dunér F, Patrakka J, Xiao Z, **Larsson J**, Vlamis-Gardikas A, Pettersson E, Tryggvason K, Hultenby K, Wernerson A.
Dendrin expression in glomerulogenesis and in human minimal change nephrotic syndrome. *Nephrol Dial Transplant*. 2008;23(8):2504-11.
- II) Perisic L, Lal M, **Hulkko J**, Hultenby K, Önfelt B, Sun Y, Dunér F, Patrakka J, Betsholtz C, Uhlen M, Brismar H, Tryggvason K, Wernerson A, Pikkarainen T.
Plekhh2, a novel podocyte protein downregulated in human focal segmental glomerulosclerosis, is involved in matrix adhesion and actin dynamics. *Kidney Int*. 2012;82(10):1071-83.
- III) **Jenny Hulkko**, Jaakko Patrakka, Mark Lal, Karl Tryggvason, Kjell Hultenby and Annika Wernerson.
Neph1 is reduced in primary Focal Segmental Glomerulosclerosis (FSGS), Minimal Change Nephrotic Syndrome (MCNS), and corresponding experimental models adriamycin (ADR) mice and puromycin aminonucleoside (PAN) rats. *Nephron Extra* 2014;4:146-154.
- IV) **Jenny Hulkko**, Anna Levin, Julia Wijkström, Liqun He, Peter Barany, Annette Bruchfeld, Johan Nordström, Maria Herthelius, Jenny Nyström, Jaakko Patrakka, Miyuki Katayama, Christer Betsholtz, Kjell Hultenby, Annika Wernerson.
Nuclear translocation of Dendrin in IgA nephropathy. 2015. Manuscript.

2 CONTENTS

Abstract.....	5
1 List of Publications.....	7
2 Contents.....	8
3 List of abbreviations.....	10
4 Background.....	11
4.1 The normal kidney.....	11
4.1.1 Structure.....	11
4.1.2 Function.....	13
4.1.3 The glomerular filtration barrier.....	14
4.1.4 Filtration.....	16
4.1.5 The podocyte.....	16
4.1.6 The slit diaphragm.....	18
4.2 Pathology.....	20
4.2.1 Proteinuria and foot process effacement.....	20
4.2.2 Podocytopenia and glomerulosclerosis.....	23
4.2.3 Focal Segmental Glomerulosclerosis.....	24
4.2.4 Minimal Change Nephrotic Syndrome.....	25
4.2.5 IgAN nephropathy.....	26
4.2.6 IgA vasculitis.....	27
4.2.7 Membranous Nephropathy.....	27
4.2.8 Experimental animal models.....	28
4.3 Genetic analysis techniques.....	29
5 Aim.....	32
6 Ethical considerations.....	33
7 Material.....	35
7.1.1 Human, normal renal tissue used as controls.....	35
7.1.2 Patients.....	35
7.1.3 Biopsy material.....	35
7.1.4 Adriamycin Nephropathy (ADR).....	36
7.1.5 Puromycin aminonucleoside nephropathy (PAN).....	36
7.1.6 Gene expression profiling with Affymetrix.....	37
7.1.7 Expression constructs.....	37
7.1.8 Cell cultures, transient and stable transfections.....	37
8 Methods.....	39
8.1 Immunohistochemistry.....	39
8.1.1 Primary antibodies.....	39
8.2 Tissue preparation.....	40
8.2.1 Tissue preparation for light microscopy.....	40
8.2.2 Immunofluorescence, human material.....	40
8.2.3 Immunofluorescence, cultured cells.....	40
8.2.4 Drug treatment of cells.....	41
8.2.5 Immunoperoxidase staining.....	41
8.3 Electron microscopy (EM).....	42
8.3.1 Tissue preparation for transmission electron microscopy ..	42

8.3.2	Immuno Electron Microscopy (iEM)	42
8.3.3	Semiquantification of structural proteins by iEM	43
8.3.4	Yeast two-hybrid screening	44
8.3.5	Western blotting	44
8.3.6	Co-immunoprecipitations	45
8.3.7	Fluorescent Resonance Energy Transfer (FRET)	45
8.3.8	In vitro actin polymerization and depolymerization assays	46
8.3.9	Live cell imaging (Article II, supplementary)	46
8.3.10	Glomerular microdissection	46
8.3.11	Microarray analysis	47
8.4	Data collection and statistics	48
9	Results	49
9.1	Main findings study I	49
9.2	Main findings study II	50
9.3	Main findings study III	51
9.4	Main findings study IV	53
10	Discussion	55
10.1	Reflections on methods	55
10.1.1	Strengths/ Weaknesses of methods	55
10.2	Reflections on results	57
10.2.1	Study I and IV	57
10.2.2	Study II	58
10.2.3	Study III	59
6	CONCLUSION	61
7	Clinical significance	64
9	Acknowledgements	65
10	References	67

3 LIST OF ABBREVIATIONS

BSA= Bovine Serum Albumin

FPE= Foot Process Effacement

FSGS= Focal Segmental Glomerulosclerosis

GBM= Glomerular Basement Membrane

HSP= Henoch–Schönlein purpura

iEM= Immuno Electron Microscopy

IgAN= IgA Nephropathy

IgAV= IgA Vasculitis

IFL= Immunofluorescence

MCNS= Minimal Change Nephrotic Syndrome

MN= Membranous Nephropathy

PB= Phosphate buffer

PAS= Periodic-Acid Schiff

PASM= Periodic Acid Silver

SD= Slit Diaphragm

TEM= Transmission Electron Microscopy

4 BACKGROUND

4.1 THE NORMAL KIDNEY

4.1.1 Structure

The normal human kidney measures about 12 cm. Blood from the abdominal aorta enters the kidneys via the renal arteries. Structurally the kidney is composed of an outer cortex and an inner medulla. The kidneys' functional units are called nephron. A normal human kidney has approximately 1 million nephrons, composed of a glomerulus and tubular system (Figure 1). The glomerulus consists of small capillary bundles, held together structurally and functionally by mesangial cells and their matrix; all encapsulated by Bowmans capsule (Figure 2-4) which is connected to the tubular system.

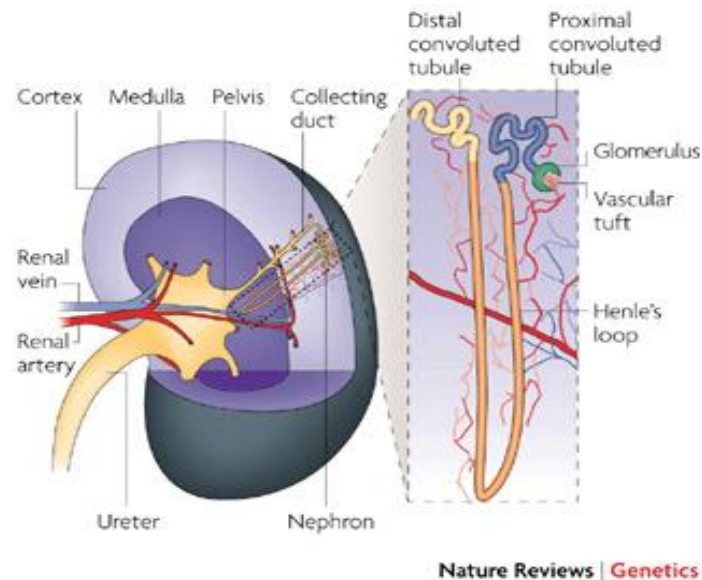


Figure 1. Structure of the normal human kidney.
Copyright © 2007, Rights Managed by Nature Publishing Group.

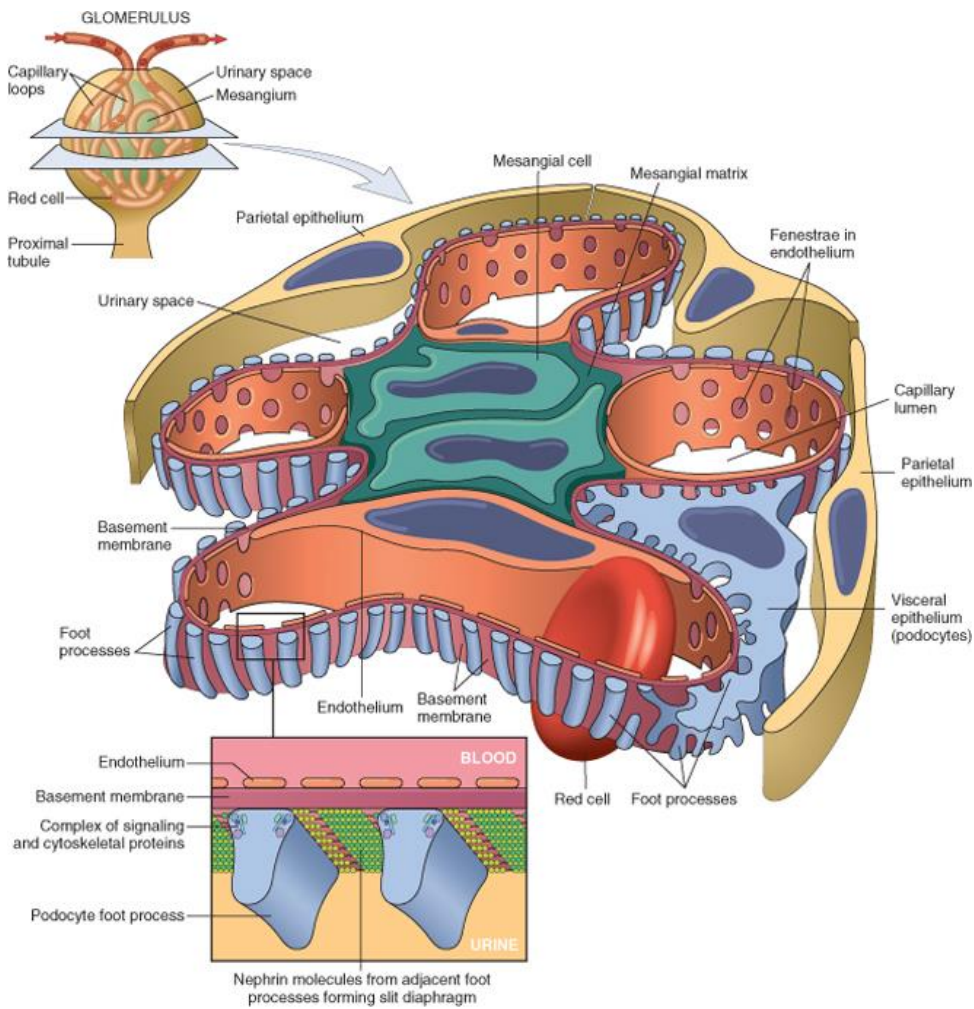


Figure 2. The glomerular filtration barrier. Copyright © 2009, Rights Managed by Nature Publishing Group.

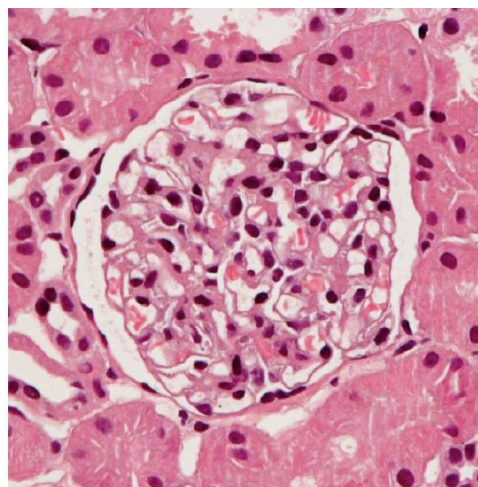
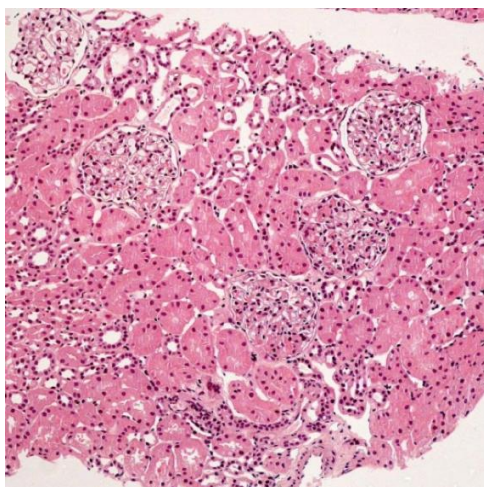


Figure 3a. Light microscopy image of normal glomeruli. Figure 3b. Light microscopy image of normal glomerulus.

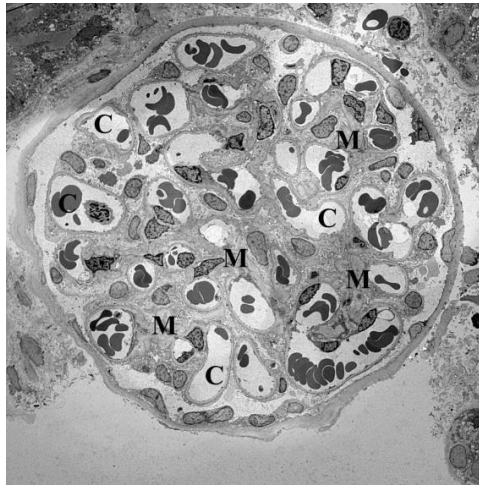


Figure 4. Electron microscopy image of a normal glomerulus. C= capillaries, M=mesangium.

4.1.2 Function

The kidneys main functions are clearing the blood from waste products and regulating the water fluid levels. Blood enters the glomerulus via the afferent (inward) arteriole. Filtered blood then leaves the glomerulus through the efferent (outgoing) arteriole. The filtration product, the primary urine, is normally free from proteins and blood cells and measures about 180 liter/day. Most of this liquid is reabsorbed in the tubular system and the amount of urine will be about 1.5 liter / day.

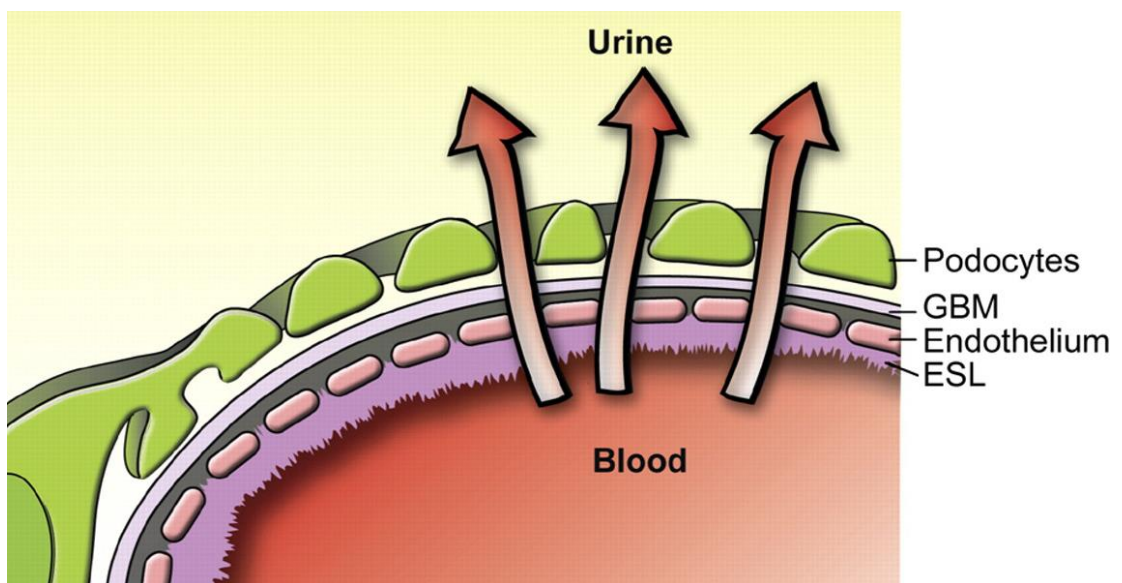


Figure 5. The blood is filtered through the glomerular capillaries, over the three layers of the filtration barrier. The product, the primary urine is collected in the Bowmans capsule before it enters the tubular system. Copyright © 2008, American Physiological Society.

4.1.3 The glomerular filtration barrier

Three core constituents build up the filtration barrier of the glomerular capillaries: the endothelium, the glomerular basement membrane (GBM) and the visceral epithelial cells, the podocytes (Figure 2, 5, 6 and 7). Compounds of low molecular weight and small size, such as water, urea and glucose readily pass the filtration barrier. Albumin and other large proteins (≥ 80 KDa) are hindered to prevent macromolecular leakage from the blood to the filtrate. The primary urine is collected in the Bowman's capsule before it enters the tubular system for further re-absorption of fluids.

The first layer, the fenestred endothelium has a negatively charged cell surface glycocalyx, containing proteoglycans and sialo proteins. Due to great difficulties to culture endothelial cells without shifting their phenotype, they are not very well studied in comparison to the other components of the filter. Also, the endothelial layer has not been considered essential to the selective glomerular filtration, mainly because of its large fenestrae. It is now, however, recognized that the endothelial cell coat has charge-selective properties (1, 2) and that the cell is bound non-covalently to the surface which means that the layer is much less permeable than previously believed. Numerous current studies present data that highlights the endothelium as a perm-selective layer (1, 3, 4, 5).

The mayor components of the second layer, the 300-350 nm GBM, are type-IV collagen and $\beta 2$ -laminin, interconnected by nidogen and agrin. The GBM is not generally regarded as the main barrier of neither size nor charge selection. This has been shown by studies on the selective removal of highly anionic substances, which appears to neither influence the glomerular charge selectivity nor increase the degree of proteinuria (6).

The outer wall of the capillaries, facing Bowman's capsule, consists of podocytes with cell bodies and foot processes (Figure 6). Filtration slits, spanned by porous slit diaphragms (SD), are located between neighboring foot processes (Figure 6). Both podocytes and endothelial cells adhere to the adjacent mesangial extracellular matrix (ECM). Through connecting surface receptors the cells and the ECM together regulate growth, differentiation and survival (7, 8) of the glomerular components.

Recently a location between the podocytes and the basement membrane was described. This so called sub-podocyte space (SPS) covers approximately two thirds of the

basement membrane and allegedly regulates protein transfer to Bowmans space through exit pores (9).

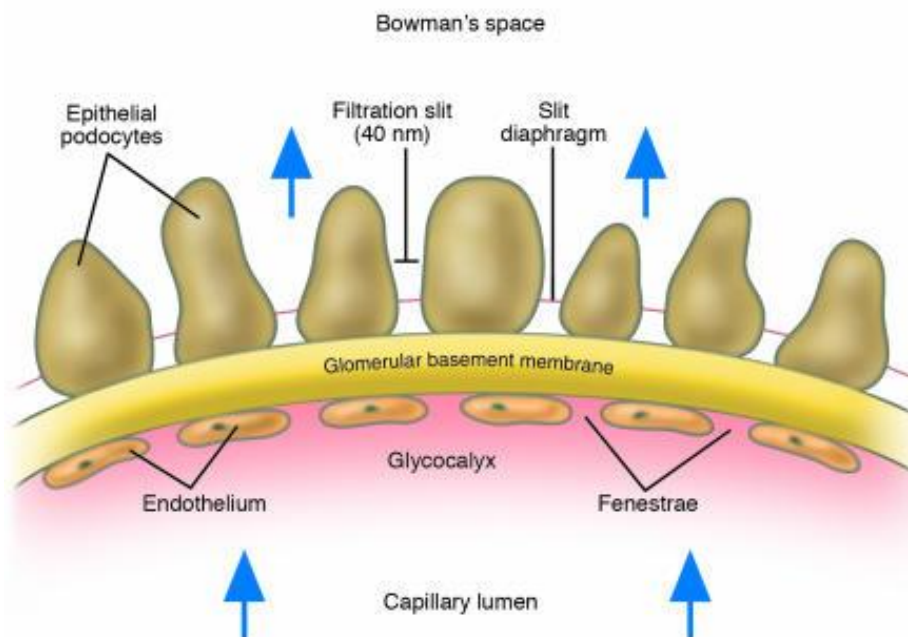


Figure 6. The epithelial podocytes with foot processes and intermediate slit diaphragms. Copyright, © 2004 American Society for Clinical Investigation.

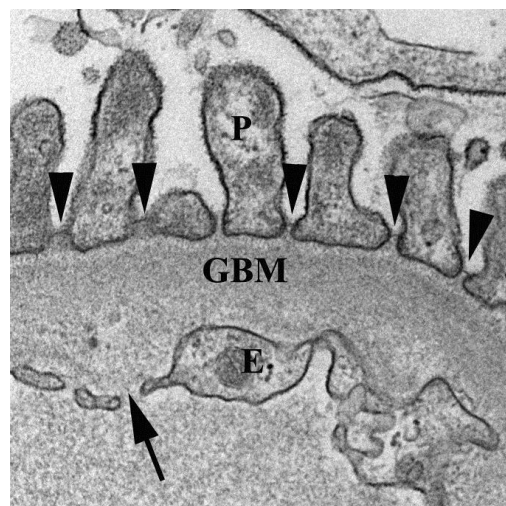


Figure 7. Electron microscopy image of the glomerular filtration barrier. E= endothelium, GBM= glomerular basement membrane, P= podocytes.

4.1.4 Filtration

Until recently the general idea was that glomerular filtration is driven by diffusion and convection (by the flux of water). It seems, however, as electrokinetic effects are involved. Briefly, the ionic plasma fluid interacts with the charged filter walls when passing the glomerular filter. Menzel et al (10) calculated the sum of these interactions. The fact that anions pass the glomerular filter slightly faster than cations, generate an electrical potential across the filter, directly proportional to filtration pressures.

A pronounced mystery of the glomerular filtration is that despite the fact that more than 99.9% of the 7 kg plasma proteins filtered every day is retained by the filter, the filter is never clogged. This has led to the hypothesis that most plasma proteins are excluded from the filtrate before it reaches the SD.

Numerous mechanisms have been proposed, as summarized by Haraldsson et al (1, 2), including: ingestion of proteins by mesangial cells, GBM charge repulsion, a hypothesis governing gel infusion and endocytotic transport of albumin to the podocytic cytoplasm and excretion in Bowmans space (11).

In 2011 Menzel et al (10) suggested that the energy potential derived from albumin and most plasma proteins negative charge will induce an electrophoretic flux, toward the blood, which will transport these macromolecules from the filter back into the blood. Positively charged components will in turn, be transported from the filter into the urine by diffusion, convection, and electrophoresis. The required energy is supplied by the blood pressure. The podocytes main function in the filtration process would thus, based on this hypothesis, be as generators of a potential difference.

4.1.5 The podocyte

Podocytes are allegedly terminally differentiated cells. They *can* enter the cell cycle but has a very limited capacity of complete cell division. It is still not known if and how podocytes can be substituted (12). Two mechanisms proposed:

1. Stem cell migration via the blood from the bone marrow, which has been demonstrated in experimental systems (13).
2. Migration of the parietal epithelial cells layering Bowmans capsule to the glomerular tuft, and thereafter a phenotype differentiation (14).

The highly specialized podocyte consists of a cell body, major processes, secondary processes and foot processes. The cell body, the secondary and major processes are constructed primarily of intermediate filaments which maintain the shape, and by microtubules which provide the dynamics of the cytoskeleton. The foot processes contain long actin filaments that connect adjacent processes, and are anchored to the underlying basement membrane through transmembrane receptors, such as integrins, tetraspanins and dystroglycans. The integrins are, in turn, linked to the podocyte actin cytoskeleton. The cell membrane of the foot processes is divided into three domains: the apical membrane domain, the SD and the basal membrane domain (15). The basal membrane domain is attached to the GBM and all three domains are linked to the actin cytoskeleton.

The actin ability to swiftly polymerize and de-polymerize allows morphological changes of the foot processes. Regulation of the cytoskeletal dynamics is crucial to the normal podocyte function.

The podocytes both retain the structure of GBM and produce many of its components, for example heparan sulphate proteoglycans. Damage to the podocytes disturbs this symbiosis. A thickening of the GBM due to the podocytes increased production of matrix protein is seen in the glomerular disease Membranous Nephropathy (MN). The podocytes also affect the endothelial cells by the production of vascular endothelial growth factor (VEGF) and angiopoietin, which regulate the fenestration of the endothelial cells and is essential for their development (16).

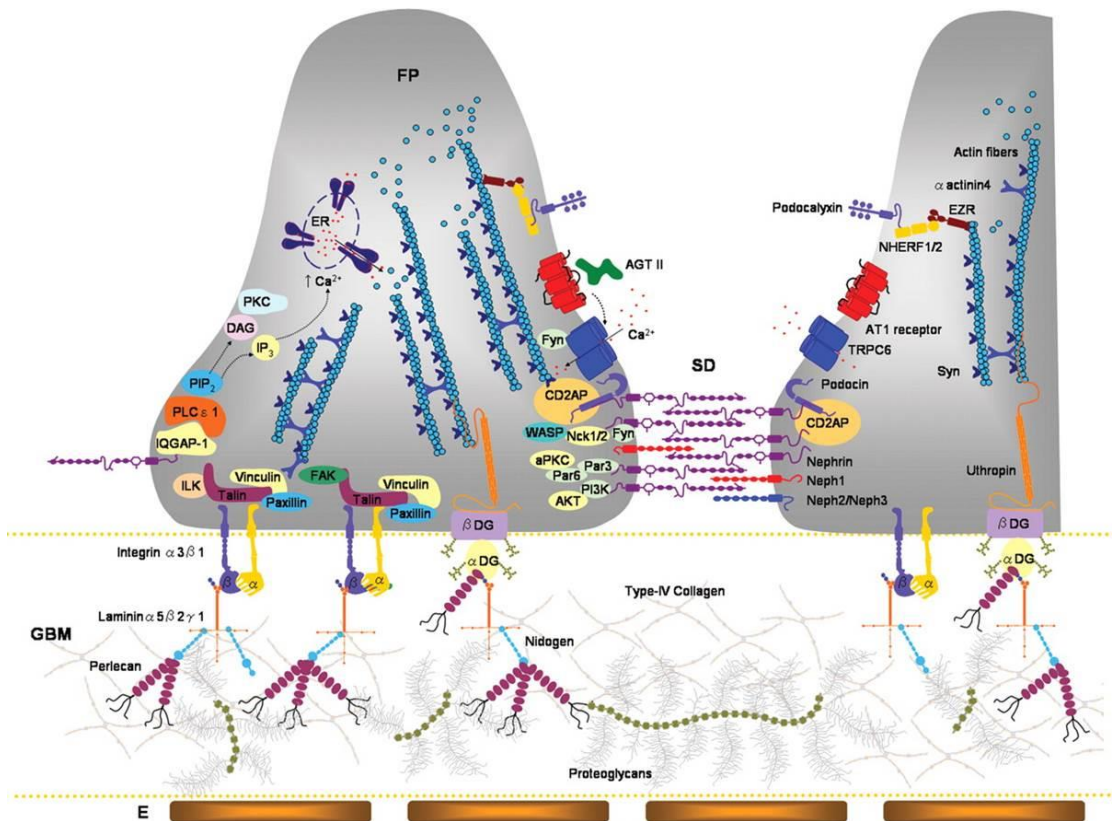


Figure 8. Adjacent foot processes and the intermediate slit diaphragm. Copyright © 2009, Oxford University Press.

4.1.6 The slit diaphragm

Adjacent foot processes interdigitate through 25-60 nm slit diaphragms (SD), functioning both as charge and size selective barriers and as platforms connected to the intracellular cytoskeleton by signaling pathways (Figure 8 and 9). The morphological structure of the SD resembles desmosomes and adherens junctions. The slit diaphragm was first described by Karnovsky in 1974 in mice and rats (17) and the following year in humans (18). That same year the SD also reported to be lost in areas of foot process effacement in Minimal Change Nephrotic Syndrome (MCNS) and restored after steroid treatment (19). In 1998 Tryggvason et al. identified the protein Nephrin as a major component of the SD (20). By positional cloning, a mutation in its encoding gene, *NPHS1*, could be linked to congenital nephrosis of the Finish type (20), a condition characterized by heavy proteinuria in utero. These findings led to the notion that structural changes of the SD and the podocyte cytoskeleton are involved in nephrotic diseases. It is now recognized that SD proteins, for example Nephrin (20), Neph1 (21), Podocin (22), P-cadherin (23), and FAT (24), are linked to the podocyte

cytoskeleton through adaptor proteins (25), such as CD2-associated protein (CD2AP) (26, 27), Zonula Occludens (ZO)-1 (28), β -catenin, Nck and p130Cas (29) (Figure 8). The adaptor proteins, in turn, interact either directly with actin or indirectly through actin-binding proteins, such as β -actinin, Synaptopodin, Cofilin or Fimbrin (29). The morphological structure, polarity and function of the foot processes are thus controlled by the extracellular SDs transmission of signals (30) to the intracellular actin cytoskeleton (Figure 9). For example, Podocin and TRPC6 are believed to function as sensors of mechanical stress and pressure from filtration, and contribute, through signaling cascades, to resulting rearrangements of the cytoskeleton (31, 32). Further, phosphorylation of the proteins involved in the signaling pathways of the SD function as on/off settings of the podocytic response to external provocations (33). New genes of the SD are continuously being identified and associated with human proteinuric disease, the latest being; APOLI, PTPRO, COQ26, INF2 and MYO1E (33). The exact molecular construction of the SD is to this day unestablished.

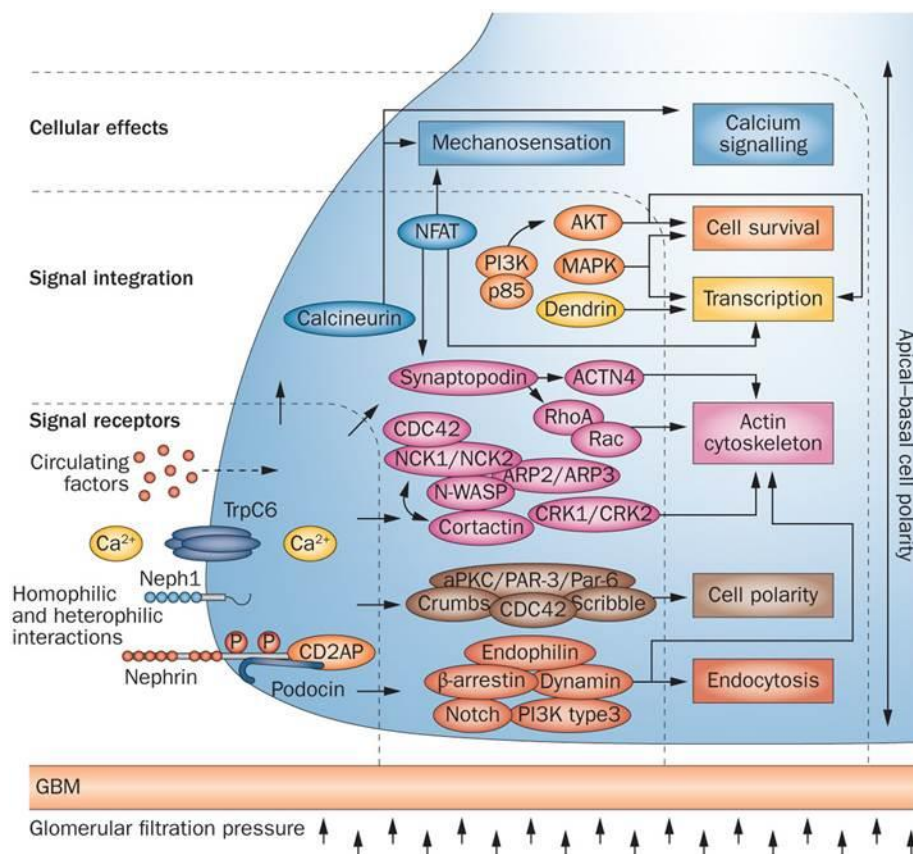


Figure 9. Signaling pathways at the slit diaphragm. Copyright © 2013, Rights Managed by Nature Publishing Group.

4.2 PATHOLOGY

The prevalence of chronic kidney disease (CKD) is approximately 10% globally (34). As a consequence of the increased incidence of type 2 diabetes and an ageing population, the number is predicted to rise even further the forthcoming years. Chronic kidney disease eventually leads to renal failure, requiring dialysis or transplantation. Following Diabetic Nephropathy and hypertonia, glomerulonephritis is the most common cause of chronic kidney failure, and counts for 25% of the cases (34, 35). Due to limited knowledge of the pathogenic mechanisms behind acquired glomerular diseases, the therapies offered today are unspecific and sometimes even harmful.

4.2.1 Proteinuria and foot process effacement

Urinary protein excretion is considered normal up to 150 mg per day, with albumin excretion below 30 mg. When the urinary protein concentration measures $\geq 3,5$ g protein/24h it is diagnosed as proteinuria, - the most common sign of renal disease and glomerular dysfunction. Extensive protein leakage is in itself harmful to the kidney (36), and also an independent risk factor for cardiovascular mortality (37). Proteinuria is caused by the dysfunction of the selective permeability through the filtration barrier, or an impairment of the tubular reabsorption, but the molecular mechanisms are not known (38). The combination of pronounced proteinuria (>3.5 g protein/24h), hypoalbuminuria, oedema and hyperlipidemia is referred to as nephrotic syndrome. Several mutations of podocyte associated proteins have been identified in hereditary proteinuria, from those related to the slit diaphragm, cell matrix, cytoskeleton and podocyte surface, to transcriptional factors, and podocyte-secreted proteins (39). For example: CD2AP (25), α -actinin-4 (40), Transient Receptor Potential Channel 6 (TRPC6) (41), Podocin (42), and most recently Myosin 1E (MYO1E) in childhood-onset steroid resistant nephrotic syndrome (43). Functional loss of SD-associated Nephrin, Podocin and TRCP6 channels has been shown to be involved in the onset of proteinuria in acquired glomerular diseases (44). However, the maintenance of glomerular function requires working collaboration between all present cells, not just podocytes, but also endothelial, mesangial and

parietal epithelial cells. Therefore proteinuria should be considered a defect of the filtration barrier as a whole, occurring regardless of which glomerular compartment that is injured (1, 16, 45). There are numerous mutations of GBM proteins associated with proteinuria, such as collagen type IV and laminin, as well as the endothelial glycocalyx association to albuminuria in type 1 diabetes (46). Furthermore, deficiency of $\alpha3\beta1$ -integrins separates the foot processes from the GBM and induces proteinuria (47). There are also circulation factors and signaling pathways known to be associated to proteinuria: such as angiotensin II, VEGF, calcium (48) and Rho GTPase signaling (15).

A characteristic ultrastructural finding in nephrotic syndrome and proteinuric diseases is so called foot process effacement (FPE), as first described by Farquar in 1957 (49). This re-arrangement of the cytoskeletal parallel actin filaments into a compressed network (Figure 10 and 11), is the podocytes adaptive response to injury or stress (33, 50). At the initial stage the foot processes retract into short projections, which, at the second stage are further withdrawn into the primary podocyte cell processes and finally, fuse with the cell bodies. The podocyte cell bodies are by then covering the GBM by direct adherence (50).

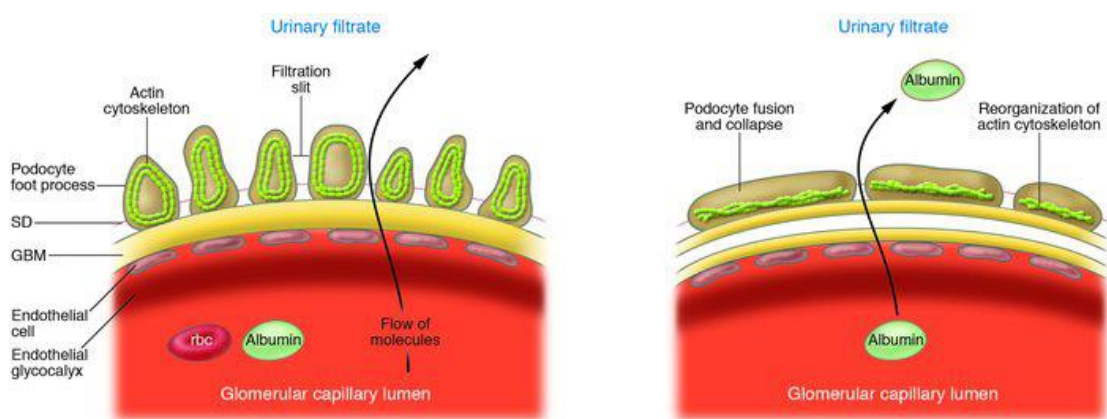


Figure 10. Normal foot processes (left) and effaced foot processes (right). Copyright © 2000, Journal of Clinical Investigation.

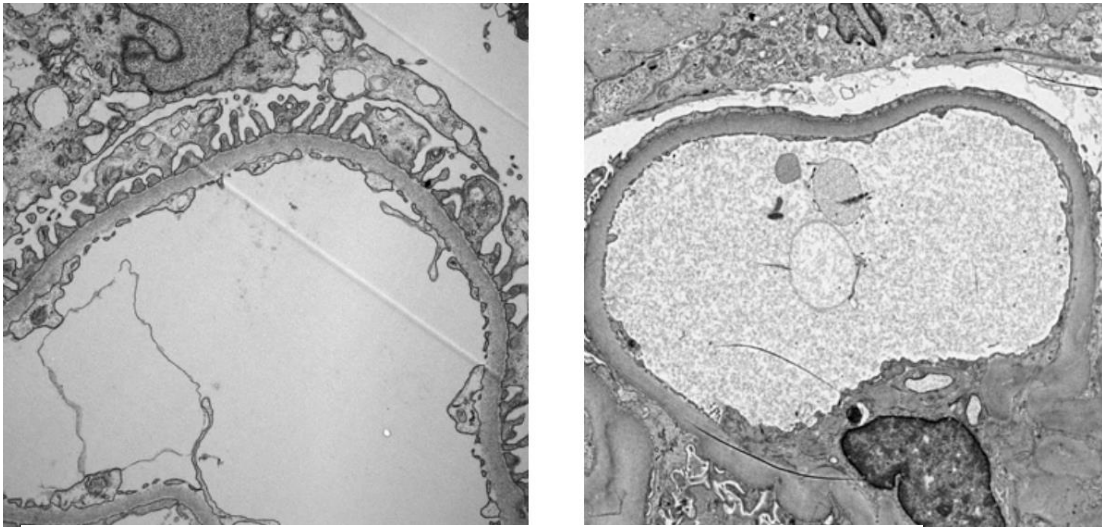


Figure 11a. Electron microscopy image of normal glomerular capillaries. Figure 11b. Electron microscopy image of foot process effacement in MCNS.

The glomerular injury resulting in FPE, may be caused by toxins or viruses, metabolic diseases (e.g. diabetes), immunological responses/defects, genetic mutations, ischemia or abnormal glomerular hemodynamic forces (51, 14). Podocytes with effaced foot processes commonly form long apical microvilli which attach to the GBM or to the parietal basement membrane (PBM). This act has been described as the podocytes pursuit for new attachment sites (50).

When rapid polymerization of the actin cytoskeleton is required due to damage or development, Neph1 is phosphorylated and recruits adaptor protein Nck, which in turn activates actin. Neph1 is also known to be phosphorylated in injured glomeruli, but the exact signaling pathway remains to be defined (52). The polymerization of the actin cytoskeleton is a reversible event, which has been successfully shown in a number of animal studies (53) and is also seen in the glomerular disease Minimal Change Nephrotic Syndrome (see below) following treatment. Confusingly, the SD shift towards tight junction formation, which is seen as a result of FPE, would rather prevent proteinuria. Effacement in itself does not seem to be sufficient to cause proteinuria, as proteinuria can occur without FPE, and the degree of FPE does not correlate to the amount of proteinuria (54, 55). Although still extensively debated, the general belief is currently that proteinuria and FPE are two independent symptoms of glomerular injury. Indeed, in 2010 Gagliardini et al (56) closely examined the pores of the SD with scanning EM, and could thereby describe them as heteroporous instead of the previously proposed zipper-like structure. They also found significantly larger pores in

rats with proteinuric pathologic conditions, than in controls. This, they suggested, could explain proteinuria with unchanged foot process morphology.

An alternative theory governing glomerular filtration and proteinuria is the notion that the proximal tubule retrieves proteins that are filtered through the glomerulus by transcytosis, and that defects of this reuptake mechanism are responsible for proteinuria (57).

Kriz and colleagues (50) recently suggested that FPE is the podocytic strategy to escape detachment from the GBM, following injury. In order of doing so, the podocytes form a temporary basis that enables reconstruction of the filtration barrier when possible.

Thus, the effacement of the foot processes would also aim to limit protein leakage by preventing podocyte detachment. This would imply that measuring urinary podocytes would be a far better marker of disease severity and treatment response than proteinuria. The authors do acknowledge that many genetically induced disorders and some acquired diseases would be excluded from this theory, where the FPE is triggered as a result of specific mutations rather than as a response to injury.

4.2.2 Podocytopenia and glomerulosclerosis

A significant factor in the progression of proteinuric kidney diseases to kidney failure is podocytopenia, the loss of podocytes. The depletion can either be caused by direct loss by apoptosis, necrosis, autophagy or detachment, or by glomerular enlargement resulting in indirect podocyte loss (14) (Figure 12). Detachment of podocytes is most abundantly preceded by FPE, as the primary reaction to insult (50).

Based upon the study of rat models, the consequences of different degrees of podocytopenia have been recognized (58, 59). If the initial glomerular insult does not result in podocyte depletion, the glomerulus may repair and return to normal function. Though, following >20% podocyte loss, the glomerular capillary loop adhere to Bowmans capsule. 20-40% podocyte loss results in segmental sclerosis and >60% leads to a glomerulus with global sclerosis and no filtration function. Proteinuria develops correspondingly (58, 59).

Glomerular enlargement, associated to for example obesity and acromegaly, is another contributor to glomerulosclerosis (60).

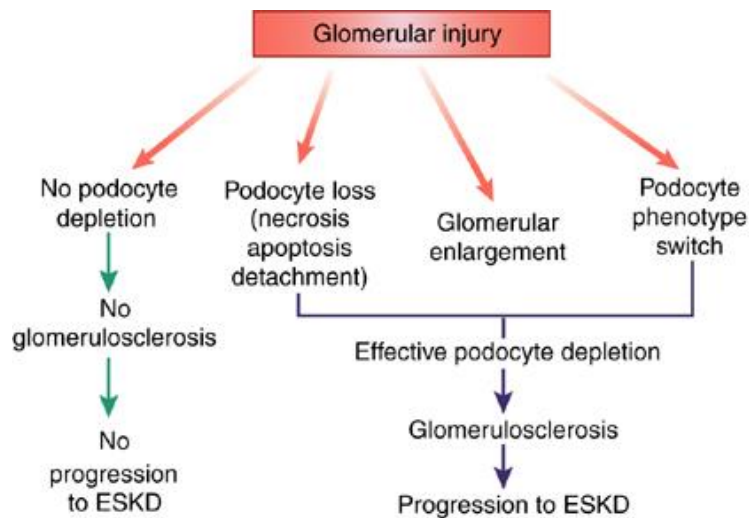


Figure 12. The podocyte depletion theory. Copyright © 2007, Rights Managed by Nature Publishing Group.

4.2.3 Focal Segmental Glomerulosclerosis

Focal Segmental Glomerulosclerosis (FSGS) is the primary glomerular disorder that most commonly result in end stage renal disease in the United States (61). The disease manifests with proteinuria, glomerular lesions of focal and segmental sclerosis and FPE (Figure 13). In contrast to Minimal Change Nephrotic Syndrome (see below), the effacement seen in FSGS is not readily reversed. FSGS can be of either primary or secondary type. Secondary FSGS have an underlying cause, such as virus-or drug-association, heritability or can be mediated by adaptive structural-functional responses, such as renal dysplasia or obesity.

The disease is primarily a histological diagnosis, based on the presence of segmental sclerotic lesions involving some, but not all glomeruli. Ever since the first portrayals of the disease by Fahr and Rich in 1925 and 1957 respectively, several different types of FSGS have been described (62-64) and numerous attempts at classification have been made. According to the pathologic classification system of Colombia (65, 66), FSGS include five different subclasses based on the presence of histological features; cellular, tip lesion, perihilar, collapsing and not otherwise specified (NOS). Based upon this classification system, the perihilar type is characterised by sclerosis and/or hyalinosis in the perihilar region of the glomerulus. The cellular, tip and collapsing variants must be

excluded. The tip lesion variant should have at least one glomerulus with defining features of segmental lesion involving the glomerular tip domain and adhesion or confluence of glomerular tuft lesion in the tip domain. The lesion may be sclerosis, endocapillary hypercellularity or foam cells. In our second study we used the perihilar and tip lesion types as these are the most common primary variants of FSGS in our region.

The significance of distinguishing between these histological types of FSGS clinically has been debated, but numerous studies (67-69) have demonstrated considerable differences in both clinical features and renal outcome between the histological types. As earlier discussed, podocytopenia can lead to sclerosis, but it is not known whether all identified mutations in hereditary FSGS, such as α -actinin-4 (40, 70), Podocin (71), CD2-associated protein (CD2AP) (72), TRPC6 (73, 74) and Inverted Formin 2 (INF2) (75), lead to podocyte loss or target the podocyte structure through other mechanisms. Idiopathic, primary FSGS is presently thought to be the result of circulating permeability factors, such as soluble urokinase-type plasminogen activator receptor (suPAR) (76) and cardiotrophin-like cytokine-1 (CLC-1) (77).

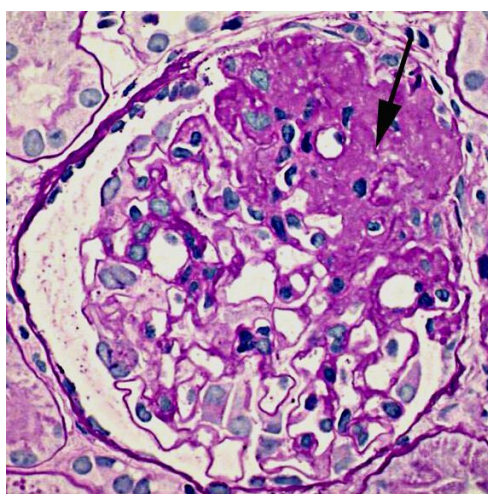


Figure 13. Light microscopy image of FSGS. PAS staining of a glomerulus with a segmental sclerosis (Arrow).

4.2.4 Minimal Change Nephrotic Syndrome

Minimal Change Nephrotic Syndrome (MCNS) shares the most prominent clinical manifestations with FSGS, such as severe FPE and proteinuria – however, with normal appearance in light microscopy, as opposed to the focal, segmental glomerulosclerosis that characterizes FSGS. The use of transmission electron microscopy (TEM) to

identify FPE is therefore a helpful tool in analyzing biopsy material (Figure 11). MCNS is the most common disease underlying nephrotic range proteinuria among children. It is typically activated by immunological events, such as allergy. The podocytic injury in MCNS, resulting in the characteristic FPE is thought to be caused by a circulating factor secreted by abnormal T cells (78). Treatment with glucocorticoids does indeed swiftly restore the normal podocyte shape and glomerular function. In 2003, we presented reduced Nephlin expression in the podocytes of MCNS patients (79).

CD80, a transmembrane protein involved in T-cell activation has recently been shown to be significantly increased in MCNS compared to FSGS (80). Hopes are that this could be the long sought factor distinguishing MCNS from FSGS in a simple urine test. Prior to this study there were some discussions regarding the staining of CD80/B7-1 in glomerulopathies (81) and whether the results were merely artefacts of cross-reactivity (82).

4.2.5 IgAN nephropathy

IgA nephropathy (IgAN) was first described by Berger and Hinglais in 1968 (83), and is the most common primary glomerulonephritis worldwide. The disease is immunohistologically defined by the presence IgA deposits, which has been shown to be galactose deficient, within the glomerular mesangium (61). Further, mesangial cell proliferation and matrix expansion is seen, resulting in a reduction, and eventually occlusion, of the capillary lumen and glomerulosclerosis.

Clinically, IgAN patients may present with hypertension, hematuria with or without proteinuria of various degrees (84). The fact that the intensity of the deposits and the severity of glomerular injury do not correlate, is extensively studied. The detailed immunological mechanism behind glomerular IgA deposits is still unidentified. Some therefore believe IgAN to be a collection of different diseases, sharing the deposits but not the underlying pathology (85). The degree of glomerulosclerosis seems to correlate to podocyte depletion, and IgAN patients along with MN patients (see below), show an increase of excreted podocytes in urine (86, 87). Segmental sclerosis in IgAN may be a result of healed necrotizing lesions, leaving segmental scars (88).

In 2009 the collaboration of the International IgA Nephropathy Network and the Renal Pathology Society published two papers describing their new IgAN Oxford Classification (89, 90). With the aim to identify specific pathological features predicting the progression risk of the disease in individual IgAN cases, they presented four variables of independent value: (1) mesangial hypercellularity, (2) segmental glomerulosclerosis, (3) endocapillary hypercellularity, and (4) tubular atrophy/interstitial fibrosis. However, the prognostic value of the classification system has since then been challenged (88, 91- 94).

4.2.6 IgA vasculitis

IgA vasculitis (IgAV) (formerly known as Henoch Schönlein purpura) is an acute immunoglobulin A (IgA)–mediated disorder, mainly affecting children. It is characterized by vasculitis involving the small vessels of the skin, the gastrointestinal tract, the kidneys and the joints. The renal involvement with IgA deposits in vascular walls and/or in glomeruli correlates to the long term prognosis. Clinically, the patients show microscopic hematuria and low-grade proteinuria. The etiology and pathogenesis are unknown, but the disease seems to be associated to, and induced by infections, in particular of the upper respiratory tract (95).

4.2.7 Membranous Nephropathy

Membranous Nephropathy (MN) patients typically show proteinuria, edema, hypoalbuminemia, and hyperlipidemia. The disease can be of either primary or secondary origin, and is the most common idiopathic nephrotic syndrome in white adults. Underlying causes of secondary types of MN are autoimmune diseases, infection, drugs, and malignancy (96). 30-40% of the patients progress toward end-stage renal failure within 5 to 15 years (97).

MN is immunologically mediated and forms glomerular sub-epithelial immune-complex deposits with subsequent thickening of the glomerular basement membrane.

The immune complexes lead to glomerular damage through activation of the complement pathways.

The factor most often associated with idiopathic, primary MN is autoantibodies against endogenous anti-phospholipase A₂ receptor (anti-PLA₂R) (98). New antigen candidates are continuously being reported, such as human leukocyte antigen (HLA) complex class II HLA-DQ alpha chain 1 (HLA-DQA1) (99) and superoxide dismutase 2 (100, 101). Most recently detected in MN are autoantibodies against thrombospondin type-1 domain-containing 7A (THSD7A) (102).

4.2.8 Experimental animal models

Animal models are an indispensable tool for studying the mechanisms of FPE, proteinuria and the function of specific proteins in the glomerular filtration barrier. Above all, they enable insights of the different stages of proteinuria and FPE, from the onset and early stages, to fully developed disease. Based upon the area of interest there are now a vast number of different animal models available, for example Heymann's nephritis with formation of in situ immune complex, models of hyperfiltration due to reduced number of nephrons and neutralization of the podocytes glycocalyx, resulting in FPE (103). Last year a murine line consistently developing IgAN was designed (104).

For our studies, we used two non-transgenic animal models of nephrotic syndrome; puromycin aminonucleoside (PAN) administration to rats, and adriamycin administration (ADR) to mice. The podocytes are toxically injured in both models. Puromycin interrupts the ribosomal protein translation and adriamycin leads to DNA inserts, both substances resulting in considerable proteinuria. Obviously, great caution must be taken when translating results from animal models to human pathology.

4.3 GENETIC ANALYSIS TECHNIQUES

The introduction of next-generation sequencing (NGS) has truly revolutionized genetic testing in research and diagnostics. The techniques can be used to identify novel genes, link single-nucleotide polymorphisms (SNPs) to specific diseases and also provide information of the gene functions (105).

The traditional DNA Sanger-sequencing is a highly sensitive tool for identification of mutations, but is most successfully used to detect disease genes already known. In order to analyze genetically heterogeneous diseases, the method would be extremely time consuming and expensive. Next-generation sequencing, on the other hand, are able to analyze multiple genes or even complete genomes within days.

Next-generation sequencing involves sequencing techniques of variously sized targets and resulting data; from *whole-genome sequencing* and *whole-exome sequencing* to *targeted sequencing* which sequences specifically selected parts of the genome and *gene panel sequencing* of selected known and candidate disease-causing genes (106).

Most commonly used is whole-exome sequencing. The method combines specifically targeted protein-coding DNA with massively parallel sequencing, resulting in the complete coding variation of an individual genome. Thus, this method has hugely enhanced the discovery of genes linked to, for example, nephrotic syndrome (107).

Single nucleotide polymorphism (SNP) microarray analysis can be used to identify homozygosity in the genome and differences in gene copy numbers. Based upon this primary regional demarcation, the chosen area can then be more closely analyzed by NGS techniques.

Chromatin immunoprecipitation with sequencing (ChIP-seq) perform genome wide analysis and detects transcriptional DNA-binding sites and histone modifications that are known to regulate gene expression. In contrast to array techniques, ChIP-seq is not limited by fixed ranges of probe sequences. The method only requires a small amount of DNA for analysis and do not involve the troublesome hybridization step. However, ChIP-seq relies on PCR amplification to detect visible signals and is expensive.

Transcriptome profiling using RNA-sequencing (RNA-seq) can identify and position mRNA, non-coding RNA, and small RNA and further detect and quantify posttranslational modifications.

Hopes are that the methodological development of NGS in combination with the continuous identification of disease-linked genes, will lead to more specifically targeted therapies.

5 AIM

With the aim to characterize the function of novel glomerular proteins in the human glomerulus, a genomic-, proteomic-, and bioinformatic research program was launched by groups at KI and KTH. By collaboration with these groups, we have access to antibodies against newly identified glomerular proteins. The specifically produced antibodies, in combination with the biopsy material from the hospital's bio bank offers a unique possibility to study the expression of novel proteins in the renal filtration barrier in normal and diseased kidneys.

With the hypothesis that the molecular structures of the podocytes and SD are altered in proteinuric diseases with foot process effacement, we wanted to study the localization and distribution of specific structural proteins in the normal kidney and in glomerular disease. The novel glomerular proteins included in this thesis: Dendrin, Plekhh2 and Neph1.

6 ETHICAL CONSIDERATIONS

Normal renal tissue was taken from unaffected kidneys that had been surgically removed because of localized carcinoma (study I-III) and from living, healthy kidney donors (study IV).

All biopsies were taken for diagnostic purposes and re-examined to confirm the diagnosis.

The material is used in agreement with the local ethical board.

(Dnr 1395–32/2005, 2010/579-31/1, 2014-2210-32).

All animal experiment were conducted according to Swedish animal research regulations and approved by the local Board of Ethics.

(D228/99, 1395-32/2005, S65/2001, S25/2002, S209/03 N250/11)

PRESENTATION OF THE STUDIES

This thesis is composed of four articles, three published and one manuscript.

Study I describes the cytosolic podocyte protein Dendrin, which previously have been identified in the brain and in mouse podocytes, associated to the actin cytoskeleton. As the regulation of the podocyte actin cytoskeleton is of considerable interest in glomerular diseases with FPE, we wanted to study the expression of Dendrin in MCNS. The expression of the protein Zona Occludens-1 (ZO-1), known to be localized close to the SD, was included for comparison.

Study II focuses on the intracellular protein Plekhh2, an uncharacterized protein with strongest expression in the podocytes and in the testis. Zebra fish *PLEKHH2* knock-downs have shown changes in the capillary walls with thickening of the GBM and disorganization of the foot processes. The aim of this study was to identify interaction partners of Plekhh2, as these interactions are likely to indicate the proteins physiological functions, and to investigate the expression of Plekhh2 in human proteinuric disease.

Study III examines the transmembrane protein Neph1 that forms a complex with Neph1 in the SD. With recent indications of the involvement of the Neph1-Neph1 complex in actin polymerization and in proteinuria, we wanted to study the expression of Neph1 and compare it to that of Neph1 in FSGS and MCNS, and in their corresponding experimental models Adriamycin Nephropathy (ADR) and Puromycin aminonucleoside nephrosis (PAN).

Study IV returns to Dendrin. We semi-quantified nuclear Dendrin in renal biopsies from patients with IgA nephropathy (IgAN) (including IgAV) and Membranous Nephropathy (MN) using iEM, and analysed the glomerular gene expression with microarray. This study was inspired by recent findings of an increased occurrence of Dendrin-positive podocyte nuclei in IgAN, evaluated by immunofluorescence (IFL).

7 MATERIAL

7.1.1 Human, normal renal tissue used as controls

Study I-III: normal renal tissues from unaffected parts of kidneys surgically removed because of localized carcinoma.

Study IV: biopsy material from living, healthy kidney donors. The biopsy was taken immediately after the kidney was removed from the donor.

7.1.2 Patients

Patients, who fulfilled the criteria of MCNS, FSGS, IgAN, IgAV and MN clinically and histopathologically, were chosen for the studies. Classification of FSGS was performed according to the Columbia system (65, 66). For study II we used the perihilar and tip lesion types as these are the most common variants of primary FSGS in our area. The IgAN cases were classified according to the Oxford system (89, 90) based upon the presence of mesangial hypercellularity, segmental glomerulosclerosis, endocapillary hypercellularity, tubular atrophy/interstitial fibrosis, and additionally for presence of cellular or fibrocellular crescents

7.1.3 Biopsy material

All biopsies included in the studies were taken for diagnostic purposes. Immediately after the biopsy was taken, the material was evaluated by an experienced technician. Material for light microscopy, immunofluorescence and electron microscopy were prioritized as the histopathological diagnosis is based on these examinations (see below). If possible, e.g. if the biopsy material was large enough, small pieces of tissue were embedded for iEM. Recently we have been able to collect patient material for gene expression analyses, as discussed later.

7.1.4 Adriamycin Nephropathy (ADR)

Adriamycin Nephropathy is a well-established experimental animal model of human FSGS (103). The administration of the toxin adriamycin leads to a progressive, chronic glomerular disease, characterized by proteinuria, segmental glomerulosclerosis, FPE and tubulointerstitial fibrosis. Formerly being a model based upon rats, Wang et al published a protocol for mice in 2000. The ADR method has greatly enhanced the understanding of the processes underlying the progression of renal injury (108). In our material (Study III) we could measure extensive albuminuria day 7 after injection, along with partial FPE. By day 14, segmental sclerotic lesions were present in the glomeruli of all animals except for one. This material allowed us to study the protein expression in the initial phase, as well as in fully developed disease with sclerotic lesions of the glomeruli.

7.1.5 Puromycin aminonucleoside nephropathy (PAN)

Puromycin aminonucleoside is an antibiotic originating from the *Streptomyces alboniger* bacterium. Intravenous administration of the toxin results in proteinuria and FPE (109). PAN is believed to be converted by the podocyte xanthine oxidase to a toxic metabolite, leading to glomerular injury. In contrast to ADR it does not give rise to segmental sclerosis of the glomeruli until after 16 weeks, and is therefore used as an experimental model of MCNS.

In our material (Study I, III), partial FPE was seen by day 2 after injection, before the onset of proteinuria by day 4. The FPE was widespread by day 4. No sclerotic lesions were present in the glomeruli (110).

We used material from day 2 in order to study the protein expression prior to proteinuria and the material from day 4, presenting both proteinuria and FPE, as a comparison to human MCNS material.

7.1.6 Gene expression profiling with Affymetrix

Two mouse glomerular disease models were included in this analysis:

Lipopolysaccharide (LPS)-induced nephrotic syndrome, a sub-septic mice model of transient proteinuria (111) and type II diabetic mice model (Norlin J. et al, manuscript). Mouse glomerular RNA was isolated and hybridized on Affymetrix arrays and the array data were processed as described before.

7.1.7 Expression constructs

Expression constructs were generated by the cloning of PCR-amplified fragments into various expression vectors. Inserts were amplified from kidney cDNA (Mouse MTC Panel I, Clontech Laboratories, Palo Alto, CA) with Long PCR Enzyme Mix (Fermentas International, Burlington, Canada), and sequenced to confirm the absence of PCR-generated mutations. The PCR program used was as follows: 1 cycle of 95°C/4 min, 30 cycles of 95°C/1 min, 51°C/1 min, 72°C/2–10 min, and 1 cycle of 72°C/10 min. For yeast two-hybrid screening, inserts were cloned into the vector pGBKT7 (Clontech Laboratories) in frame with the Gal4 DNA-binding domain. For expression in mammalian cells, cDNAs were cloned into pcDNA3.1 (Invitrogen, Carlsbad, CA), or vectors with various N-terminal tags (pCMV-Myc, pCMVHA, or pEGFP-C; all from Clontech Laboratories).

7.1.8 Cell cultures, transient and stable transfections

Human podocytes were grown at 33°C/5% CO₂ in RPMI supplemented with 10% fetal bovine serum (Invitrogen), 1x insulin-transferrin-selenium-A supplement (Invitrogen), and antibiotics (100 U/ml penicillin and 100 µg/ml streptomycin) (Invitrogen), as previously described. HEK293, COS7, NIH3T3 and CHO cells were cultured at 37°C/5% CO₂ in DMEM containing the same supplements, except ITS-A. Cells were transiently transfected with Lipofectamine 2000 (Invitrogen) according to the manufacturer's recommendations. For generation of stable-expressing HEK293 clones, cells were selected and maintained in medium containing 500 µg/ml of G418. Stable

transfectants were characterized by GFP immunofluorescence and Western blotting for GFP expression.

8 METHODS

8.1 IMMUNOHISTOCHEMISTRY

Immunohistochemistry is used to define the localization of a biochemically defined antigen, i.e., to localize a specific protein in tissue or cell with an antibody directed towards the antigen.

In order for the antibody to recognize the antigen in the tissue structure, it is of foremost importance that the protein structure is preserved as intact as possible.

8.1.1 Primary antibodies

In the preparation of polyclonal antibodies, the specific protein is biochemically isolated and injected in the animal. The immune response from the B-cells gives a large amount of antibodies directed towards *different* epitopes of the antigen, i.e. polyclonal antibodies. The IgG fraction (most commonly) is then filtered out for production. To produce monoclonal antibodies, *one (1)* specific B cell is isolated and cloned to produce antibodies directed against the same, specific, epitope.

For immunohistochemistry (especially iEM) studies, polyclonal antibodies are preferred as the probability of one specific epitope, being exposed on the surface of the embedded tissue is very low. If the antibodies are directed against a number of epitopes, the probability of binding the specific protein increases.

8.2 TISSUE PREPARATION

8.2.1 Tissue preparation for light microscopy

Specimens were fixed in 4% phosphate buffered formaline, dehydrated and embedded in paraffin according to standard procedures. 1.5 μm sections were cut on a microtome, and stained with hematoxylin-eosin, periodic-acid Sciff (PAS), Ladewig trichrome, and periodic acid silver (PASM).

8.2.2 Immunofluorescence, human material

An unfixed piece of the renal biopsy taken for diagnostic purposes was snap frozen. For diagnostic purposes, 5 μm thick cryosections were incubated with FITC-conjugated antibodies against IgG, IgA, IgM, fibrinogen, the light chains kappa and beta and the complement factors C3 and C1q.

For our studies of novel glomerular proteins, the cryosections were postfixated with cold acetone (-20°C) and blocked in 5% normal goat serum. Primary antibodies were incubated overnight at 4°C and the secondary fluorescent antibody for 1 hour in darkness, in room temperature.

8.2.3 Immunofluorescence, cultured cells

Cells were grown on fibronectin-coated glass coverslips. For coating, coverslips were incubated with 10 mg/ml of fibronectin (Invitrogen, 33010-018) for 2 h at room temperature, followed by several washes with phosphate-buffered saline (PBS). Cells were fixed with 4% paraformaldehyde solution for 20 min at room temperature, after which they were permeabilized by incubation with 0.1% Triton X-100/PBS for 5 min, followed by an incubation with 2% bovine serum albumin/PBS (blocking solution) for 1 h. In some experiments, cells were treated with 0.5% saponin/PBS for 20 min before fixation. After blocking, cells were incubated with primary antibodies for 1 h at room temperature, washed several times with PBS, and then incubated for 1 h with a suitable

secondary antibody. All antibodies were diluted in the blocking solution. Secondary antibody solutions also contained rhodamine–phalloidin and 4,6-diamidino-2-phenylindole to stain F-actin and cell nuclei, respectively. For double labeling, incubations were performed sequentially to prevent cross-reactions. Photos were taken using Zeiss LSM510 confocal microscope, with X 20, X 40, or X 63 objectives.

8.2.4 Drug treatment of cells

Transiently transfected human podocytes were plated on fibronectin-coated coverslips in 24-well plates, and left to adhere and spread for 16 h. Thereafter, cells were incubated for 1 h at 37°C with 100 nmol/l of wortmannin (Sigma, W1628) or 50 mmol/l LY294002 (Cell Signaling, 9901), inhibitors of phosphatidylinositol 3-kinase, or 10 mg/ml of the actin monomer–sequestering drug latrunculin A (Sigma, L5163), all diluted from stock-solutions prepared in dimethylsulfoxide. Control cells were incubated with the vehicle only. After the incubation, cells were fixed and stained for Myc-tagged Plekh2 and F-actin as described above.

8.2.5 Immunoperoxidase staining

2, 5 µm sections of paraffin-embedded tissue were pre-treated with tris-EDTA (Dako, Glostrup, Denmark) followed by 3% H₂O₂ in methanol. 10% milk was used as blocking for 30 minutes. The primary antibody, or normal IgG as negative control, was incubated overnight after which the HRP-conjugated secondary antibody (Envision TM, Dako, Glostrup, Denmark) was added for 30 minutes at room temperature and then visualized by the DAB/ H₂O₂ substrate. Nuclei were stained by hematoxylin.

8.3 ELECTRON MICROSCOPY (EM)

The resolution in light microscope is limited by the wavelength of the light (350-700 nm). Replacing light by electrons (0,002 nm) gives better resolution and the possibility to study the ultrastructure of the tissue. Compared to the 5000 nm tissue sections that can be examined with light microscopy, the EM equivalents are as thin as 50 nm and the resolution is approximately 0,1 nm, in contrast to the 300 nm of LM.

Electron microscopy is a black and white technique. In order to identify structures, the contrast in the tissue material must be enhanced.

Tissue used for TEM requires a special fixation and embedding protocol.

8.3.1 Tissue preparation for transmission electron microscopy

Tissue were fixed in a phosphate buffered 2% glutaraldehyde, and post-fixed in osmium tetroxide (O_5O_4) in order to enhance contrasts. After alcohol dehydration followed by acetone, the specimen were embedded and polymerized in a plastic resin to enable the ultrathin sectioning of approximately 40- 60 nm. The specimen were then mounted on a formvar coated grid and finally contrasted by adding the heavy metals, lead citrate and uranyl acetate.

8.3.2 Immuno Electron Microscopy (iEM)

Small pieces of tissue were dehydrated at low temperature in methanol and embedded in Lowicryl K11M (Chemische Werke Lowi, GmbH, Waldkreiburg, Germany), a special resin which enables iEM. Ultrathin sections were mounted on carbon/formvar nickel grids and incubated in 2% bovine serum albumin (BSA) and 2% gelatin in 0.1 M phosphate buffer (PB) at pH 7.4 followed by incubation overnight with primary antibodies (Dendrin, Plekhh2, Neph1 and Nephrin), diluted 1:100 and 1:50 respectively, in 0.1M PB containing 0.1% BSA and 0.1% gelatin (PBBG). Bound antibodies were detected by protein A conjugated with 10 nm colloidal gold (Biocell Laboratories Inc., Rancho Dominguez, CA, USA), diluted 1:100 in PBBG.

When double staining Neph1 and Neph1rin, Neph1rin was incubated overnight, followed by Neph1 for 3 hours. Secondary antibodies conjugated with 5 nm and 10 nm gold particles respectively were used to detect the bound antibodies.

8.3.3 Semiquantification of structural proteins by iEM

The primary antibody is detected by protein A molecule tagged with a 10 nm gold particle which, due to its high density, allows visualisation by electron microscopy. Protein A derives from *Staphylococcus Aureus* and is used because of its specific binding to the Fc part of the IgG molecule. Protein A binds to the IgG molecule in the ratio of 1:1, thereby allowing semi-quantification. Protein A also gives lower background compared to the use of secondary antibodies which can bind multiple epitopes of the IgG molecule.

Sections were examined in a Tecnai 10 microscope (FEI Company, the Netherlands) and digital images were taken by a Veleta camera (SiS Company, Münster, Germany).

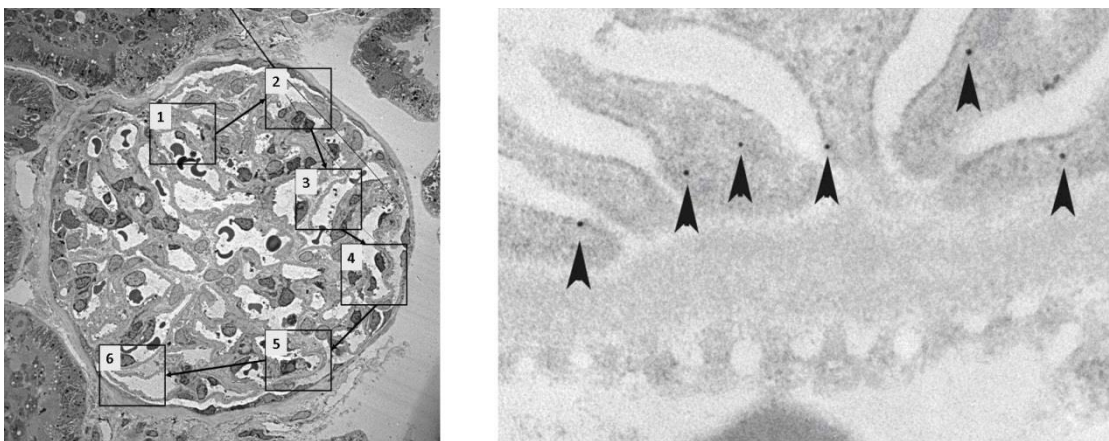


Figure 14a. Semi quantification by iEM. Six locations of the glomerulus were chosen according to a random systematic sampling procedure. 14b. Gold markers identified in the podocytes.

Six locations per glomerulus (1–2 glomeruli, depending on material) were chosen with a random start at low magnification along the glomerular capillaries. Three images were systematically taken from each location, including areas with or without foot process effacement (no sclerotic areas), giving a minimum of 18 images/specimen (Figure 14a). Prints at a final magnification of 52 000 \times were examined and the number of gold

markers (Au) was counted in the podocytes, GBM and endothelial cells, respectively. In study IV, a minimum of 8 images/biopsy were also taken of the podocytes nuclei. The area of the different compartments were calculated by point counting, using a 1×1 cm square lattice (112), and expressed as μm^2 . Dividing the total number of gold particles by the area, give the concentration ($\text{Au}/\mu\text{m}^2$) (Figure 14b). In order to distinguish between areas with and without FPE, the length of the GBM was measured and the number of slits/ μm GBM calculated. Less than 1 slit/ μm GBM was defined as FPE.

8.3.4 Yeast two-hybrid screening

For yeast two-hybrid screening, we used a mouse kidney glomerulus cDNA library custom-generated by Clontech. The library was screened with baits encoding the Gal4 DNA-binding domain fused to full-length Plekhh2 or its deletion variants. Screening was carried out by yeast mating according to the manufacturer's instructions. Diploids were selected through several rounds of culture on minimal synthetic dropout medium. Plasmids from obtained colonies were isolated, sequenced, and analyzed with the BLAST algorithm at the National Center for Biotechnology Information (NCBI).

8.3.5 Western blotting

Western blot separates proteins based on molecular weight through gel electrophoresis. The proteins are then transferred from the gel of the electrophoresis to a membrane where they can be bound, and thereby identified, by specific antibodies. This binding is then visualized by exposure of the membrane in a dark room. The amount of protein can be estimated by the thickness of the band seen.

Western blotting for the Plekhh2 study was carried out following standard procedures.

8.3.6 Co-immunoprecipitations

Confluent transiently transfected HEK293 cells were washed twice in cold PBS and lysed in 0.5% Triton X-100, 20 mM Tris-HCl (pH 7.4) and 150 mM NaCl buffer containing protease inhibitor cocktail (Roche) and phosphatase inhibitors (1 mM NaVO₃, 50 mM NaF). Lysates were clarified by centrifugation (14000 x g), incubated with primary antibodies overnight, followed by an incubation with protein A+G agarose beads (Roche Molecular Biochemicals) for 1 h at 4°C. Thereafter the beads were washed 3 times with the lysis buffer, resuspended in 1x SDS-sample loading buffer, and boiled for 10 min. Eluted proteins were analyzed by SDS-PAGE and Western blotting. For subcellular fractionation experiments, cell lysates were fractionated with Qproteome Cell Compartment Kit (Qiagen) prior to gel analysis.

8.3.7 Fluorescent Resonance Energy Transfer (FRET) in fixed cells

A detailed description of the FRET technique can be found elsewhere (113). We utilized this method to confirm dimerization of the Plekhh2 protein using human podocytes cotransfected with GFP- and Myc-tagged versions of Plekhh2. The Förster constant, R₀, for the donor-acceptor pairs used in this study, Alexa488 and Alexa568, is 62Å. To determine FRET, we quantified the quenching of donor fluorescence by performing acceptor photobleaching. FRET measurements were performed using a Zeiss LSM510 inverted confocal microscope, apochromat 63x/1.4 NA oil immersion objective and the Zeiss LSM510 software version 2.8. Briefly, fluorophores were excited with 488 and 543 nm laser and images collected separately. The acceptor, Alexa568, was then irreversibly photobleached in a selected adequate region by continuous excitation with a 543 nm laser for about 30 s. Thereafter, residual Alexa568 and Alexa488 image was obtained under same settings as prebleach images, and identical regions on individual cells were outlined in the photobleached area and processed using ImageJ. Ratios between Alexa488 intensities of the selected region, after and before photobleaching, were calculated to quantify FRET. In a typical experiment 15–20 cells were measured for each sample.

8.3.8 In vitro actin polymerization and depolymerization assays

In vitro actin polymerization and depolymerization assays using the Actin Polymerization Kit (Biochem) were employed to study the role of Plekhh2 in the actin assembly processes. The assay relies on the difference between fluorescent signals of pyrene-labeled monomeric G-actin and polymerized pyrene-F-actin (used as positive controls in our experiments). For these assays, we used lysates prepared from 293 cells stably expressing GFP-Plekhh2, and control cells. Cells were plated onto plates coated with 10 µg/ml of fibronectin, and allowed to adhere overnight in a serum-free media, followed by an overnight treatment with medium containing 10% FCS or 30 µg/ml of PDGF-BB (Invitrogen). After this, cells were collected and lysed for 3 h at 4°C in a buffer containing 20 mM Tris-Cl, pH 7.5, 20 mM NaCl and protease inhibitors. Lysates were clarified by centrifugation at 14000 rpm for 50 Perisic!Ljubica 50 10 min. The actin polymerization and depolymerization assays were performed according to manufacturer's instructions, and fluorescence kinetic measurements were done with TECAN GENiosPro.

8.3.9 Live cell imaging (Article II, supplementary)

Imaging of GFP-Plekhh2-expressing human podocytes plated on fibronectincoated glass coverslips was started immediately after cell plating. Imaging was continued overnight, with images being taken every 5 min (Zeiss LSM 510 microscope, 40 X objective). They were then processed into a movie with the ImageJ program.

8.3.10 Glomerular microdissection

Immediately after biopsy procedure, the renal tissue material was placed on a drop of RNA Later. The material was then placed in the fridge for a minimum of 24 hours and thereafter in a – 20 or -80 degrees Celsius freezer. The glomeruli were isolated from the renal tissue under a dissection microscope and placed on a drop of RNA Later. The glomeruli were transferred to an Eppendorf tube containing 350 µl RLT lysis buffer

(Qiagen, Netherlands). 3,5 µl β-mercaptoethanol was added, and the sample vortexed for 1 minute. The sample was then quick-frozen.

8.3.11 Microarray analysis

The total RNA from microdissected glomeruli was extracted using RNeasy® Mini Kit (Qiagen, Netherlands). Microarrays were performed on human genome U133 plus2.0 array (Affymetrix, Santa Clara, Calif., USA) by the Bioinformatics and Expression Analysis Core Facility (BEA) at Karolinska Institutet using standard protocols.

8.4 DATA COLLECTION AND STATISTICS

The material used for iEM must be saved and embedded prospectively. Thus, such material can only be prepared if the biopsy is large enough to still allow a proper histopathologic examination. This means that for material from a certain disease we must both rely on the biopsy quality, the amount of material from the biopsy, and the general prevalence of the specific disease in our area. The relatively small number of cases representing each specific disease can be rather troublesome when it comes to statistics.

9 RESULTS

9.1 MAIN FINDINGS STUDY I

In normal renal tissue, IFL showed Dendrin in almost complete overlap with Nephtrin (used as an SD marker) in a linear pattern along the glomerular capillaries. With EM we could localize 36% of Dendrin close to the SD.

Neither the staining pattern nor the intensity of Dendrin or ZO-1 differed between MCNS and controls, using IFL. This was confirmed by iEM. No significant change in the total amount of Dendrin or ZO-1 was seen in MCNS compared to controls, neither in areas with or without FPE (Table 1). Both Dendrin and ZO-1 were redistributed from the SD to the podocyte cytoplasm in FPE areas. The amount of Dendrin in the nuclei of PAN was unchanged compared to controls (Table 2).

Dendrin expression in the podocytes in human kidney

	Slits/ μm	Au/ μm^2	Au/slit	Percentage of Au on slits
Controls (n=5)	$1,8 \pm 0,3$	$1,2 \pm 0,4$	$0,1 \pm 0,0$	36 ± 12
MCNS, areas with FPE (n=5)	$0,5 \pm 0,1$	$0,9 \pm 0,3$	$0,1 \pm 0,1$	$17 \pm 9^*$
MCNS, areas without FPE (n=5)	$1,6 \pm 0,3$	$1,5 \pm 1,0$	$0,2 \pm 0,1$	32 ± 4

Table 1. Expression of Dendrin in controls and MCNS based on iEM, gold particles/ μm^2 (Au/ μm^2). The data are presented as mean \pm sd, * = $p < 0.05$ compared to controls.

Dendrin expression in the podocyte nucleus in rat

Controls	1,2 ± 0,3
PAN	1,3 ± 0,5

Table 2. Expression of Dendrin in controls and MCNS based on immunoelectron microscopy, gold particles/ μm^2 ($\text{Au}/\mu\text{m}^2$). The data are presented as mean \pm sd.

9.2 MAIN FINDINGS STUDY II

Using IFL and iEM we localized Plekhh2 to the podocyte foot processes in the normal human glomerulus. The protein was mainly found centrally in the foot process cytoplasm (56%) or close to the plasma membrane (within a distance of 100 nm, 28%). Some expression was also seen close to the GBM (12%) but rarely in the SD. We showed that Plekhh2 is present in the membrane and cytoskeletal fractions of cultured human podocytes, which suggests that it is associated to these structures. Yeast-two hybrid (Y2H) screening identified Hic-5 and β -actin as interacting partners of Plekhh2. With iEM we could visualize the co-localization of Plekhh2 and Hic5 in the podocyte foot processes close to the GBM.

In cells treated with actin monomer-sequestering drug, Plekhh2 stabilizes the cortical actin cytoskeleton, possibly by diminishing actin depolymerization.

Semi-quantification by iEM showed Plekhh2 to be significantly reduced in primary FSGS of perihilar and tip lesion types, compared to controls. There was a re-distribution from the plasma membrane to centrally in the foot processes in the tip lesion type. This was also identified in perihilar FSGS, although not statistically significant. There was no significant change in the overall amount of Plekhh2 in MCNS and MN, except for a reduction in non-FPE areas in MCNS (data not published) (Table 3). We also found Plekhh2 to be unchanged in Diabetic Nephropathy (DN) compared to controls (Table 4). As a different batch of Plekhh2 antibodies was used for the DN cases, we calculated these separately, and compared to the controls incubated concurrently.

We found no correlation between the amount of Plekhh2 and degree of proteinuria and slits/ μm GBM (data not shown).

Plekkh2 expression ($\text{Au}/\mu\text{m}^2$) in podocytes in human kidney

	Total amount in podocytes	FPE	Non-FPE areas
Controls (n = 5)	1.8 ± 0.5	1.8 ± 0.4	-
Perihilar FSGS (n = 5)	$0.7 \pm 0.2^*$	1.2 ± 0.2	$0.7 \pm 0.2^*$
Tip lesion FSGS (n = 5)	1.1 ± 0.2	1.2 ± 0.2	$1.0 \pm 0.4^*$
MN (n = 5)	1.5 ± 0.5	2.4 ± 0.4	1.4 ± 0.4
MCNS (n = 5)	1.3 ± 0.4	2.2 ± 1.5	$1.0 \pm 0.2^*$

Table 3. Expression of Plekkh2 in controls, perihilar FSGS and tip lesion FSGS based on immunoelectron microscopy, gold particles/ μm^2 ($\text{Au}/\mu\text{m}^2$). The data are presented as mean \pm sd, * = $p < 0.05$ compared to controls.

Plekkh2	Total amount	FPE	No FPE
Controls (n = 4)	1.4 ± 0.1		
DN (n = 4)	1.2 ± 0.1	1.1 ± 0.2	1.5 ± 0.2

Table 4. Expression of Plekkh2 in controls and DN based on immunoelectron microscopy, gold particles/ μm^2 ($\text{Au}/\mu\text{m}^2$). The data are presented as mean \pm sd,

9.3 MAIN FINDINGS STUDY III

With iEM we localized Neph1 mainly to the SD in normal human, rat and mouse kidney. Double iEM staining of Neph1 and Neph1rin showed the proteins in close connection in the SD. This is, to our knowledge the first published EM image of the co-localization, and also of Neph1 in human kidney (page 149).

We found Neph1 to be significantly reduced in the podocytes both in areas with and without FPE in perihilar FSGS and in MCNS (Table 5), with iEM. This reduction was also seen in the corresponding experimental models PAN and ADR (Table 4). Neph1rin was unchanged in FSGS and ADR, both in areas with and without FPE, but reduced in MCNS and PAN (Table 6). The expressions of Neph1 and Neph1rin are compared and summarized in table 7.

Expression of Neph1(Au/ μm^2) in podocytes in human kidney

	Proteinuria (g/24h)	Total amount in podocyte	FPE	Non-FPE areas
Controls (n=5)	0	1,5 \pm 0,2	-	-
FSGS (n=5)	1 g/24 h- 8 g/24 h.	0,3 \pm 0,1*	0,3 \pm 0,2*	0,5 \pm 0,3*
MCNS (n=5)	1g/l – 27g/24 h	0,5 \pm 0,1*	0,5 \pm 0,1*	0,5 \pm 0,2*

Table 5. Expression of Neph1 in controls, FSGS and MCNS based on immunoelectron microscopy, gold particles/ μm^2 (Au/ μm^2). The data are presented as mean \pm sd, * = $p < 0.05$ compared to controls

Expression of Neph1in (Au/ μm^2) in podocytes in human kidney

	Proteinuria (g/24h, g/l)	Total amount in podocyte	FPE	Non-FPE areas
Controls (n=4)	0	2,4 \pm 0,6	-	-
FSGS (n=4)	1g/24 h- 8g/24 h.	2,0 \pm 0,4	2,3 \pm 0,4	1,4 \pm 0,0[◄]
MCNS (n=5)	1g/l – 27g/24 h	1,0 \pm 0,2*	0,9 \pm 0,2*	1,2 \pm 0,4*

Table 6. Expression of Neph1in in controls, FSGS and MCNS based on immunoelectron microscopy, gold particles/ μm^2 (Au/ μm^2). The data are presented as mean \pm sd, * = $p < 0.05$ compared to controls. ◄ = Only one observation

Summary of Neph1 and Nephtrin findings

	Neph1	Nephtrin
FSGS	↓	→
FSGS, FPE	↓	→
FSGS, Non FPE	↓	→
MCNS	↓	↓
MCNS, FPE	↓	↓
MCNS, Non FPE	↓	↓
ADR, Day 7	↓	→
ADR, Day 7, FPE	↓	→
ADR, Day 7, Non FPE	↓	→
ADR, Day 14	↓	↓
ADR, Day 14, FPE	↓	→
ADR, Day 14, Non FPE	↓	→
PAN, Day 2	↓	↓*
PAN, Day 2, FPE	→	↓*
PAN, Day 2, Non FPE	↓	↓*
PAN, Day 4	↓	↓*
PAN, Day 4, FPE	↓	↓*
PAN, Day 4, non FPE	↓	↓*

Table 7. Summary of findings based on immunoelectron microscopy.

Notes: ↓ = significantly reduced ($p < 0,05$), → = no change compared to controls.

*= Previously published (40).

9.4 MAIN FINDINGS STUDY IV

Semi-quantitatively, by iEM, we found the amount of Dendrin to be significantly increased in the podocyte nuclei in IgAN (Table 8), with and without nephrosis, compared to controls. The amount of nuclear Dendrin was unchanged between the morphologically based Oxford groups (89, 90) of mesangial hypercellularity, segmental glomerulosclerosis, endocapillary hypercellularity, tubular atrophy/interstitial fibrosis and crescents. Nuclear Dendrin was also unchanged in IgAV (Table 8).

The Dendrin expression in the podocyte cytoplasm was unchanged in IgAN as a group compared to controls. There was, however, an increase of Dendrin in the podocyte cytoplasm in IgAN cases without crescents.

The amount of nuclear Dendrin was not correlated to whether the patient had nephrosis or not, nor to renal disease progression, measured as mean loss of glomerular filtration rate (eGFR). There was however, a significant correlation between negative renal progression and the Oxford groups of mesangial hypercellularity, segmental glomerulosclerosis and tubular atrophy/interstitial fibrosis compared to the cases without these morphological characteristics.

Microarray analysis revealed a two fold increase in glomerular gene expression of Dendrin in IgAN.

Both gene and protein expression of Dendrin was unchanged in MN.

Expression of Dendrin ($\text{Au}/\mu\text{m}^2$) in podocyte nuclei and cytoplasm

Dendrin	Podocyte nuclei	Podocyte cytoplasm
Controls (n=5)	0,4 ± 0,1	1,5 ± 0,6
IgAN (n=19)	0,7 ± 0,0*	2,0 ± 1,0
IgAN with neprosis (n= 6)	0,8 ± 0,3	2,1 ± 1,4
IgAN without nephrosis (n=13)	0,7 ± 0,3	1,9 ± 0,8
MN (n=5)	0,3 ± 0,1	1,4 ± 0,5
IgAV (n=5)	0,6 ± 0,2	1,2 ± 0,6

Table 8. Expression of Dendrin in controls, IgAN and MN based on immunoelectron microscopy, gold particles/ μm^2 ($\text{Au}/\mu\text{m}^2$). The data are presented as mean ± sd, * = $p < 0.05$ compared to controls.

10 DISCUSSION

10.1 REFLECTIONS ON METHODS

10.1.1 Strengths/ Weaknesses of methods

As from study IV we have been able to use biopsy material from living, healthy kidney donors as controls. The biopsy is taken immediately after the kidney is removed from the donor, which means that ischemic damage to the material is minimized. When studying protein expression in the renal filtration barrier, EM has the great advantage over light microscopy that it can be used to closely observe specific cellular or subcellular structures. The method also enables identification of different morphological changes, e. g. differentiating between areas with and without FPE. This means that the amount of protein can be evaluated in normal and effaced areas, respectively. The iEM technique that we have developed to semi-quantify the expression of proteins is robust and well established in our department. However, due to the limited amount of specially embedded material there are sometimes statistical difficulties, as mentioned earlier.

We have recently initiated a renal project aiming to systematically collect material from patients undergoing biopsy procedure. In addition to the biopsy material, blood and urine are also collected, for analysis of known and new biomarkers. Using small pieces of the biopsy material, gene expression can be mapped with for example microarray analysis. These results of up- and down regulated genes, can then point to specific proteins worth further investigations with immuno-techniques. The constituent material of this project is still very limited but a fair number of biopsies from the most common diseases, such as IgAN and MN have been collected. These cases were indeed used for the microarray analysis of study IV.

The experimental models of PAN and ADR are valuable tools when assessing changes in protein expression in relation to proteinuria and FPE, and as supplements to human disease material. Though, it is very important that these models are not treated as representations of human glomerular diseases, and as mentioned earlier, that the results are not readily applied to human pathology. Mainly because the toxic injury of the

podocytes in these experimental models is both toxically specific and acute, which affect the molecular composition of the filtration barrier differently than in the slow chronic progression of MCNS and FSGS (103, 113).

10.2 REFLECTIONS ON RESULTS

10.2.1 Study I and IV

Considering the unchanged amount of Dendrin and ZO-1 in areas with and without FPE, the proteins are probably being redistributed from the SD to the podocyte cytoplasm, secondary to FPE. This pattern differs from our Neph1 and Neph1 results in MCNS, where both proteins are reduced in areas with FPE as well as in areas without, and therefore would be more probable key players in the processes behind FPE.

Since our first Dendrin publication, the most probable function of the protein is currently believed to be that of an apoptotic modulator in the podocytes. Recent years studies of Dendrin have focused on the fact that it seems to accumulate in the podocyte nucleus in response to glomerular injury, and its bindings to proteins associated to apoptosis.

In 2011 Asanuma et al (115) showed an accumulation of Dendrin in podocyte nuclei in ADR mice and in patients with FSGS and MN. In line with our earlier results (unchanged expression in PAN), they did not find nuclear Dendrin in MCNS patients. Kodama et al saw a similar nuclear translocation of Dendrin in patients with IgAN, evaluated by IFL (116).

This inspired us to continue our Dendrin study with IgAN patients to further examine the nuclear translocation, possible correlation to the morphology of the Oxford system and disease progression.

With unchanged Dendrin expression in the proteinuric diseases MCNS and MN and no correlation between nuclear amount and nephrosis in IgAN, we do not believe Dendrin to be associated to proteinuria.

We found Dendrin to be increased in the podocyte nuclei in IgAN, and its gene expression correspondingly up-regulated. These results support the hypothesis that the main function of Dendrin is that of an apoptotic inducer in injured podocytes, possibly linked to the development of chronic glomerular injury. The proposition by Asanuma et al (115) that nuclear Dendrin could serve as a marker of disease activity and prediction of progression to glomerulosclerosis in biopsy material is, however, not supported by

our results. Neither did we find the amount of nuclear Dendrin in the individual IgAN cases to be correlated to renal disease progression, nor to crescents. This could be due to difficulties to capture the immediate peak of nuclear translocation or ongoing fluctuations. Experimental models would make it possible to closely monitor the nuclear translocation of Dendrin in the course of glomerular injury. But, as earlier discussed, the acute and toxically known insult to the podocytes, is not a faithful model for acquired glomerular disease, in human.

10.2.2 Study II

Plekhh2 seemingly affect the foot process dynamics by attenuating actin depolymerization and thereby stabilizing the cortical cytoskeleton. Plekhh2, and the Y2H identified interaction partners Hic-5 and actin, were all downregulated in the experimental mice model lipopolysaccharide (LPS) of FPE and reversible proteinuria, which suggest involvement in this induced injury. We identified a re-distribution of Plekhh2 from the plasma membrane to centrally in the foot processes in both FSGS variants, although not statistically significant in the perihilar type.

The only previous publication of Plekhh2 indicating an involvement in human renal disease, is a study by Greene et al. (117), who found sequence variants in the *PLEKHH2* gene to be associated to development of Diabetic Nephropathy (DN). He et al (111, supplementary material) were, however, unable to replicate these results. These later findings (111) are further supported by our iEM data showing unchanged Plekhh2 expression in DN cases compared to controls (unpublished data, table 4). Though, the number of cases available was limited since biopsies are rarely performed on DN patients.

No other study on the expression or involvement of Plekhh2 in human glomerular disease has, to our knowledge, been published since.

10.2.3 Study III

The reduction of Neph1 in combination with unchanged amounts of Nephrin in FSGS could indicate a dissociation of the proteins from the complex.

Since the publication of our study, Takahashi et al (118) have found Neph1 and Nephrin to be significantly reduced in PAN, in line with our results. They showed that the IFL staining of both proteins shifted to a discontinuous pattern 1 hour after PAN injection and that the mRNA expression was reduced to undetectable levels. Treatment with Angiotensin II receptor blockade (ARB) prevented the reduction. Fascinatingly, when control rats were treated with ARB, their mRNA expression of Neph1 and Nephrin increased to 281% and 154% respectively. Exactly how the proteins are regulated and affected by Angiotensin II action will be interesting to follow.

Suvanto et al (119) have detected a 46-fold decrease of Neph1 in congenital nephrotic syndrome of the Finnish type (CNF) compared to controls, evaluated by immunoperoxidase and IFL. This being particularly interesting as the disease is caused by a mutation of the *NPHS1* gene, encoding for Nephrin. We also have indications of Neph1 being reduced in CNF but with only two cases available for iEM, we did not include these data in the article. Consequently, Neph1 could be part of the CNF pathology. Suvanto et al further, in contrast to our results, reported Neph1 to be only marginally reduced in MCNS, with and without proteinuria, evaluated from immunohistochemistry.

Despite the fact that Neph1 *-/-* mice show severe nephrotic syndrome and early postnatal lethality, no mutations in the *NEPH1* gene have been identified in human disease. However, considering the proteins wide expression pattern, involving heart, lung, placenta, brain, spleen and gut, a serious defect would probably not be compatible with life.

We aimed to expand the study of the Neph1- Nephrin complex to double and traditional IFL staining. Unfortunately we did not have frozen biopsy material of sufficient quality from FSGS patients. A further complication was that the Neph1 antibody did not work in paraffin embedded material despite numerous different protocols.

The published results on the Nephrin expression in acquired kidney diseases are rather conflicting. Patrakka et al. (120) found no change in Nephrin expression in FSGS, neither evaluated by immunohistochemistry nor at mRNA levels. Koop et al. (121) have reported the direct opposite in FSGS, a marked reduction of the Nephrin protein

and an increase at mRNA level. Kim et al. (122) concluded that the expression pattern in proteinuric diseases varies according to the severity of glomerular damage. Also, despite many attempts to portrait a correlation between the expression of Nephrin in glomerular diseases and the degree of proteinuria, the results are highly inconsistent (123).

6 CONCLUSION

The podocyte slit diaphragm, connected to the underlying GBM, and to the actin cytoskeleton, co-ordinate signals, initiated by external stimuli, that regulate the structure of the foot processes, and thereby, probably the function of the glomerular filtration barrier.

When podocytes are injured, from such as immunological, toxic, metabolic, viral, ischemic or genetic causes (14, 51), the remodeled actin cytoskeleton is visualized as retracted or extended foot processes. This architectural alteration can then either be reversed to complete recovery or worsened. Additional insults to the podocyte can result in detachment from the GBM or apoptosis (124, 125). If podocytopenia is widespread, sclerotic lesions will develop. Extensive global sclerosis might further lead to end stage kidney disease (58, 59). The exact mechanisms are, however still mainly uncharacterized, alongside most proteins and signalling pathways of the slit diaphragm.

With IFL and iEM we have localized Dendrin and Neph1 to the SD and Plekhh2 to the cytoplasm of podocyte foot processes.

At the SD, Dendrin binds Nephrin and CD2AP - an adaptor protein that can repress pro-apoptotic TGF- β signaling (126). Nephrin also binds Neph1 and Podocin, forming a transmembrane receptor complex. The cytoplasmic part of Nephrin binds intracellular adaptor proteins, such as ZO-1, CD2AP and Nck, which interacts either directly with the actin cytoskeleton or indirectly through actin-binding proteins. The extracellular domain of Nephrin interacts with other Nephrin molecules in the neighboring foot process. The genetic deletion of Neph1 and Nephrin independently, both lead to FPE, proteinuria and high perinatal mortality (38).

It has also been identified that Neph1 is phosphorylated in injured glomeruli of different in vivo models (52, 127-129).

The knowledge of the trigger behind actin transformation dynamics is very limited but the Neph1-Nephrin complex has been shown to be phosphorylated following protamine sulphate (PS) perfusion, an animal model resulting in immediate FPE (127, 130).

Additionally, the Neph1-Nephrin complex regulates the actin associated protein Cofilin-1 which is needed for the cytoskeletal reconstruction following this injury (131).

Arif et al (132) recently demonstrated that inhibition of Neph1 phosphorylation and prevented loss of Neph1 expression at the podocyte cell membrane, protected against PAN induced FPE. Impaired Nephrin-actin signaling has also been shown to inhibit the development of FPE (25). Altogether, this proposes Neph1 and Nephrin signaling as an important, if not the main, event in response to glomerular injury and inducer of cytoskeletal rearrangement through further cascade initiation.

An additional association to cytoskeletal dynamics is seen with our Plekhh2 findings. The protein seems to stabilize the cortical cytoskeleton by attenuating depolymerization, through its actin binding.

Dendrin-deficient mice show unaffected glomerulogenesis and healing process of induced glomerular injury (133). However, even though apoptosis is undeniably present during development, it is most likely that these early signaling pathways differ from those operating in the mature podocyte.

Although protein functions and signaling pathways of the SD are unraveling constantly, the complexity of the proteins interplay, signaling cross-talk and the unidentified extracellular ligands for SD proteins will continue to complicate the mapping and the understanding of podocytes in health and disease.

Different insults to the podocyte may induce diverse signaling pathways via different proteins and separate mechanisms, but still lead to similar or identical adaptations of the podocyte actin cytoskeleton. This could suggest that although the morphology is artificially identical, the underlying disease trigger could give unseen deviations that decide upon the outcome.

This is possibly highlighted by our results of a decreased amount of Neph1 in FSGS, while Nephrin is unchanged, and by the nuclear translocation of Dendrin in IgAN, but not in MN, all displaying FPE and proteinuria.

Whether the foot process effacement is a pure defense mechanism aiming to protect the barrier and prevent protein leakage as proposed by Kriz et al (50), or an altogether independent factor to proteinuria, will probably remain the perplexity of renal pathology for some time.

7 CLINICAL SIGNIFICANCE

The main purpose of this project was to increase the understanding of the renal filtration barrier and the role of structural glomerular proteins in the normal kidney and in acquired, proteinuric diseases. Increased knowledge of the mechanisms behind proteinuria and foot process effacement and the identification of the proteins involved, may sharpen our diagnostic tools in the diagnosis of kidney biopsies. The variable clinical appearance of many acquired glomerular diseases complicates today's clinical decision-making. The identification of specific proteins could for example serve as biomarkers of disease activity or progress, be used to better sub-classify glomerular diseases or to differentiate FSGS and MCNS. Ideally, the protein/s could be detected in the least invasive clinical procedure possible; in a urine sample.

The enhanced accessibility and use of Next-generation sequencing will probably vastly improve the molecular identification of these diseases. This will hopefully also facilitate the development of more targeted therapies, in contrast to the systemically immune suppression currently used.

9 ACKNOWLEDGEMENTS

I would like to express my gratitude to all those, who have helped me in my work during the years.

Firstly, to my main supervisor Annika Wernerson and my co-supervisors Kjell Hultenby, Fredrik Dunér and Jaakko Patrakka for sharing their time, knowledge and enthusiasm.

Also, so many thanks to:

Ingrid, Eva, Ewa, Anneli, Anna-Karin and Yodit of the EMIL and Pathology laboratories.
New members of the KAJA group: Anna Levin and Julia Wijkström.

Past and present colleagues and co-authors: Peter Barany, Mark Lal, Liqun He, Hannes Olauson, Marita Ward, Arja Kramsu, Monika Armuand, Filip Mundt, Katalin Dobra, Ljubica Perisic, Erna Petterson, Karl Tryggvason.

Members of the renal biopsy project.

Peter Stenvinkel, head of Division.

Bengt Lindholm, Baxter Novum.

The KI and KTH genomic-, proteomic-, and bioinformatic research program.

Karolinska Institutet, the departments of CLINTEC and LABMED, Divisions of Renal Medicine and Pathology.

Lastly, and foremost to my beloved husband Mikael and our amazing son Julius, you are my everything.

The best possible parents and siblings.

10 REFERENCES

1. Haraldsson B, Nyström J, Deen WM. Properties of the glomerular barrier and mechanisms of proteinuria. *Physiol Rev.* 2008;88(2):451-87.
2. Haraldsson B, Nyström J. The glomerular endothelium: new insights on function and structure. *Curr Opin Nephrol Hypertens.* 2012;21(3):258-63.
3. Satchell S. The role of the glomerular endothelium in albumin handling. *Nat Rev Nephrol.* 2013;9(12):717-25.
4. Jeansson M, Haraldsson B. Morphological and functional evidence for an important role of the endothelial cell glycocalyx in the glomerular barrier. *Am J Physiol Renal Physiol* 2006; 290 (1): F111–F116.
5. Ciarimboli G, Hjalmarsson C, Bokenkamp A, Schurek HJ, Haraldsson B. Dynamic alterations of glomerular charge density in fixed rat kidneys suggest involvement of endothelial cell coat. *Am J Physiol Renal Physiol* 2003; 285: F722–F730.
6. Goldberg S, Harvey SJ, Cunningham J, Tryggvason K, Miner JH. Glomerular filtration is normal in the absence of both agrin and perlecan-heparan sulfate from the glomerular basement membrane. *Nephrol Dial Transplant* 2009; 24 (7): 2044–2051.
7. Hynes RO. Integrins: bidirectional, allosteric signaling machines. *Cell.* 2002;110(6):673-87. Review.
8. Hynes RO. The extracellular matrix: not just pretty fibrils. *Science.* 2009;326(5957):1216-9. Review.
9. Neal CR, Crook H, Bell E, Harper SJ, Bates DO. Three-dimensional reconstruction of glomeruli by electron microscopy reveals a distinct restrictive urinary subpodocyte space. *J Am Soc Nephrol.* 2005 May;16(5):1223-35.
10. Menzel S, Moeller MJ. Role of the podocyte in proteinuria. *Pediatr Nephrol.* 2011;26(10):1775-80.
11. Certikova-Chabova V¹, Tesar V. Recent insights into the pathogenesis of nephrotic syndrome. *Minerva Med.* 2013;104(3):333-47.
12. Griffin SV, Petermann AT, Durvasula RV, Shankland SJ. Podocyte proliferation and differentiation in glomerular disease: role of cell-cycle regulatory proteins. *Nephrol Dial Transplant.* 2003;18 Suppl 6:vi8-13. Review.
13. Prodromidi EI, Poulsom R, Jeffery R, Roufosse CA, Pollard PJ, Pusey CD, Cook HT. Bone marrow-derived cells contribute to podocyte regeneration

- and amelioration of renal disease in a mouse model of Alport syndrome. *Stem Cells*. 2006;24(11):2448-55.
14. Wiggins RC. The spectrum of podocytopathies: a unifying view of glomerular diseases. *Kidney Int*. 2007;71(12):1205-14. Review.
 15. Faul C, Asanuma K, Yanagida-Asanuma E, Kim K, Mundel P. Actin up: regulation of podocyte structure and function by components of the actin cytoskeleton. *Trends Cell Biol*. 2007;17(9):428-37.
 16. Shankland SJ. The podocyte's response to injury: role in proteinuria and glomerulosclerosis. *Kidney Int* 2006; 69 (12): 2131–2147.
 17. Rodewald R, Karnovsky MJ. Porous substructure of the glomerular slit diaphragm in the rat and mouse. *J Cell Biol*. 1974; 60(2):423-33.
 18. Schneeberger EE, Levey RH, McCluskey RT, Karnovsky MJ. The isoporous substructure of the human glomerular slit diaphragm. *Kidney Int*. 1975; 8(1):48-52.
 19. Robson, A. M., Giangiacomo, J., Kienstra, R. A., Naqvi, S. T. & Ingelfinger, J. R. Normal glomerular permeability and its modification by minimal change nephrotic syndrome. *J. Clin. Invest*. 1974; 54, 1190–1199.
 20. Kestilä M, Lenkkeri U, Männikkö M, Lamerdin J, McCready P, Putaala H, Ruotsalainen V, Morita T, Nissinen M, Herva R, Kashtan CE, Peltonen L, Holmberg C, Olsen A, Tryggvason K. Positionally cloned gene for a novel glomerular protein nephrin is mutated in congenital nephritic syndrome. *Mol Cell* 1998; 1 (4): 574–582.
 21. Donoviel DB, Freed DD, Vogel H, Potter DG, Hawkins E, Barrish JP, Mathur BN, Turner CA, Geske R, Montgomery CA, Starbuck M, Brandt M, Gupta A, Ramirez-Solis R, Zambrowicz BP, Powell DR. Proteinuria and perinatal lethality in mice lacking NEPH1, a novel protein with homology to NEPHRIN. *Mol Cell Biol*. 2001;21(14):4829-36.
 22. Roselli S, Gribouval O, Boute N, Sich M, Benessy F, Attie T, Podocin localizes in the kidney to the slit diaphragm area. *Am J Pathol* 2002;160:131–9.
 23. Reiser J, Kriz W, Kretzler M, Mundel P. The glomerular slit diaphragm is a modified adherens junction. *J Am Soc Nephrol*. 2000;11(1):1-8.
 24. Inoue T, Yaoita E, Kurihara H, Shimizu F, Sakai T, Kobayashi T, Ohshiro K, Kawachi H, Okada H, Suzuki H, Kihara I, Yamamoto T. FAT is a component of the glomerular slit diaphragm. *Kidney Int*. 2001;59(3):1003-12. *Am J Pathol*. 2001 Dec;159(6):2303-8.
 25. George B, Holzman LB. Signaling from the podocyte intercellular junction to the actin cytoskeleton. *Semin Nephrol*. 2012;32(4):307-18. Review.

26. Shih NY, Li J, Karpitskii V, Nguyen A, Dustin ML, Kanagawa O, Miner JH, Shaw AS. Congenital nephrotic syndrome in mice lacking CD2-associated protein. *Science* 1999;286:312–5.
27. Shih NY, Li J, Cotran R, Mundel P, Miner JH, Shaw AS. CD2AP localizes to the slit diaphragm and binds to nephrin via a novel C-terminal domain. *Am J Pathol.* 2001 Dec;159(6):2303-8.
28. Schnabel E, Anderson JM, Farquhar MG. The tight junction protein ZO-1 is concentrated along slit diaphragms of the glomerular epithelium. *J Cell Biol.* 1990;111(3):1255-63.
29. Tae-Sun Ha, Roles of adaptor proteins in podocyte biology. *World J Nephrol.* 2013; 6; 2(1): 1–10.
30. Pierchala, B. A., Munoz, M. R. & Tsui, C. C. Proteomic analysis of the slit diaphragm complex: CLIC5 is a protein critical for podocyte morphology and function. *Kidney Int.* 2010; 78, 868–882.
31. Huber, T. B. et al. Podocin and MEC-2 bind cholesterol to regulate the activity of associated ion channels. *Proc. Natl Acad. Sci.* 2006; USA 103, 17079–17086.
32. Moller, C. C., Flesche, J. & Reiser, J. Sensitizing the slit diaphragm with TrpC6 ion channels. *J. Am. Soc. Nephrol.* 2009; 20, 950–953.
33. Grahammer F, Schell C, Huber TB. The podocyte slit diaphragm—from a thin grey line to a complex signalling hub. *Nat Rev Nephrol.* 2013;9(10):587-98.
34. National Kidney Foundation (World Kidney Day: Chronic Kidney Disease, 2015)
35. Svenska Njurförbundet
36. Abbate M, Zoja C, Remuzzi G. How does proteinuria cause progressive renal damage? *J Am Soc Nephrol.* 2006;17(11):2974-84.
37. Menon MC, Chuang PY, He CJ. The glomerular filtration barrier: components and crosstalk. *Int J Nephrol.* 2012;2012:749010.
38. Zhang A, Huang S. Progress in pathogenesis of proteinuria. *Int J Nephrol.* 2012;2012:314251.
39. Macé C, Chugh SS. Nephrotic syndrome: components, connections, and angiotensin-like 4-related therapeutics. *J Am Soc Nephrol.* 2014;25(11):2393-8.
40. Kaplan JM, Kim SH, North KN, Rennke H, Correia LA, Tong HQ, Mathis BJ, Rodriguez-Perez JC, Allen PG, Beggs A, Pollak MR: Mutations in ACTN4, encoding α -actinin-4, cause familial focal segmental

- glomerulosclerosis. *Nat Genet* 2000; 24: 251–256.
41. Möller CC, Wei C, Altintas MM, Li J, Greka A, Ohse T, Pippin JW, Rastaldi MP, Wawersik S, Schiavi S, Henger A, Kretzler M, Shankland SJ, Reiser J. Induction of TRPC6 channel in acquired forms of proteinuric kidney disease. *J Am Soc Nephrol* 2007; 18(1): 29–36.
 42. Boute N, Gribouval O, Roselli S, Benessy F, Lee H, Fuchshuber A, Dahan K, Gubler MC, Niaudet P, Antignac C: NPHS2, encoding the glomerular protein podocin, is mutated in autosomal recessive steroid-resistant nephrotic syndrome. *Nat Genet* 2000 24: 349–354.
 43. Mele C, Iatropoulos P, Donadelli R, Calabria A, Maranta R, Cassis P, Buelli S, Tomasoni S, Piras R, Krendel M, Bettoni S, Morigi M, Delledonne M, Pecoraro C, Abbate I, Capobianchi MR, Hildebrandt F, Otto E, Schaefer F, Macciardi F, Ozaltin F, Emre S, Ibsirlioglu T, Benigni A, Remuzzi G, Noris M; PodoNet Consortium. MYO1E mutations and childhood familial focal segmental glomerulosclerosis. *N Engl J Med*. 2011 Jul 28;365(4):295-306.
 44. Fukusumi Y, Miyauchi N, Hashimoto T, Saito A, Kawachi H. Therapeutic target for nephrotic syndrome: Identification of novel slit diaphragm associated molecules. *World J Nephrol*. 2014 Aug 6;3(3):77-84. Review.
 45. Deen WM. What determines glomerular capillary permeability? *J Clin Invest* 2004; 114: 1412–1414.
 46. Nieuwdorp M, Mooij HL, Kroon J, Atasever B, Spaan JA, Ince C, Holleman F, Diamant M, Heine RJ, Hoekstra JB, Kastelein JJ, Stroes ES, Vink H. Endothelial glycocalyx damage coincides with microalbuminuria in type 1 diabetes. *Diabetes*. 2006;55(4):1127-32.
 47. Kreidberg JA. Functions of alpha3beta1 integrin. *Curr Opin Cell Biol*. 2000 Oct;12(5):548-53. Review.
 48. Etienne-Manneville S, Hall A. Rho GTPases in cell biology. *Nature*. 2002 Dec 12;420(6916):629-35. Review.
 49. Farquhar MG, Vernier RL, Good RA. An electron microscope study of the glomerulus in nephrosis, glomerulonephritis, and lupus erythematosus. *J Exp Med* 1957; 106:
 50. Kriz W, Shirato I, Nagata M, LeHir M, Lemley KV. The podocyte's response to stress: the enigma of foot process effacement. *Am J Physiol Renal Physiol*. 2013; 15;304(4):F333-47.
 51. Barisoni L, Kopp JB. Update in podocyte biology: putting one's best foot forward. *Curr Opin Nephrol Hypertens*. 2003;12(3):251-8.
 52. Garg P, Verma R, Nihalani D, Johnstone DB, Holzman LB. Neph1 cooperates with nephrin to transduce a signal that induces actin polymerization. *Mol Cell Biol*. 2007;27(24):8698-712.

53. Seiler MW, Venkatachalam MA, Cotran RS. Glomerular epithelium: structural alterations induced by polycations. *Science*. 1975; 1;189(4200):390-3.
54. Kalluri R. Proteinuria with and without renal glomerular podocyte effacement. *J Am Soc Nephrol*, 2006. 17(9): 2383-9.
55. Van den Berg JG, van den Bergh Weerman MA, Assmann KJ, Weening JJ, Florquin S. Podocyte foot process effacement is no correlated with the level of proteinuria in human glomerulopathies. *Kidney Int* 2004; 66: 1901–1906.
56. Gagliardini E, Conti S, Benigni A, Remuzzi G, Remuzzi A. Imaging of the porous ultrastructure of the glomerular epithelial filtration slit. *J Am Soc Nephrol*. 2010;21(12):2081-9.
57. Dickson LE, Wagner MC, Sandoval RM, Molitoris BA. The proximal tubule and albuminuria: really! *J Am Soc Nephrol*. 2014 Mar;25(3):443-53.
58. Kim YH, Goyal M, Kurnit D, Wharram B, Wiggins J, Holzman L, Kershaw D, Wiggins R. Podocyte depletion and glomerulosclerosis have a direct relationship in the PAN-treated rat. *Kidney Int*. 2001;60(3):957-68.
59. Wharram BL, Goyal M, Wiggins JE, Sanden SK, Hussain S, Filipiak WE, Saunders TL, Dysko RC, Kohno K, Holzman LB, Wiggins RC. Podocyte depletion causes glomerulosclerosis: diphtheria toxin-induced podocyte depletion in rats expressing human diphtheria toxin receptor transgene. *J Am Soc Nephrol*. 2005;16(10):2941-52.
60. Fogo AB. Glomerular hypertension, abnormal glomerular growth, and progression of renal diseases. *Kidney Int Suppl*. 2000;75:S15-21. Review.
61. Snyder S, John JS. Workup for Proteinuria. *Prim Care*. 2014 Dec;41(4):719-735. Review.
62. Howie A, Brewer D. The glomerular tip lesion: a previously undescribed type of focal segmental glomerular abnormality. *J Pathol* 1984; 142: 205–220.
63. Detwiler RK, Falk RJ, Hogan SL, Jennette JC. Collapsing glomerulopathy: a clinical and pathologic distinct variant of focal segmental glomerulosclerosis. *Kidney Int* 1994; 45: 1416–1424.
64. Schwartz MM, Evans J, Bain R, Korbet SM. Focal segmental glomerulosclerosis: prognostic implications of the cellular lesion. *J Am Soc Nephrol* 1999; 10: 1900–1907.
65. D'Agati VD, Fogo AB, Bruijn JA, Jennette JC. Pathologic classification of focal segmental glomerulosclerosis: a working proposal. *Am J Kidney Dis* 2004; 43 (2): 368–382.
66. D'Agati VD, Kaskel FJ, Falk RJ. Focal segmental glomerulosclerosis. *N Engl J Med* 2011; 365(25):2398-411.

67. Thomas DB, Franceschini N, Hogan SL, Ten Holder S, Jennette CE, Falk RJ, Jennette JC. Clinical and pathologic characteristics of focal segmental glomerulosclerosis pathologic variants. *Kidney Int* 2006; 69: 920–926.
68. Deegens JK, Steenbergen EJ, Borm GF, Wetzels JF. Pathological variants of focal segmental glomerulosclerosis in an adult Dutch population--epidemiology and outcome. *Nephrol Dial Transplant* 2008; 23(1):186-92.
69. D'Agati VD, Alster JM, Jennette JC, Thomas DB, Pullman J, Savino DA, Cohen AH, Gipson DS, Gassman JJ, Radeva MK, Moxey-Mims MM, Friedman AL, Kaskel FJ, Trachtman H, Alpers CE, Fogo AB, Greene TH, Nast CC.
Association of histologic variants in FSGS clinical trial with presenting features and outcomes. *Clin J Am Soc Nephrol*. 2013;8(3):399-406.
70. Michaud JL, Chaisson KM, Parks RJ, Kennedy CR. FSGS-associated alpha-actinin-4 (K256E) impairs cytoskeletal dynamics in podocytes. *Kidney Int* 2006; 70 (6): 1054–1061.
71. Caridi G, Bertelli R, Carrea A, Di Duca M, Catarsi P, Artero M, Carraro M, Zennaro C, Candiano G, Musante L, Seri M, Ginevri F, Perfumo F, Ghiggeri GM. Prevalence, genetics, and clinical features of patients carrying podocin mutations in steroid-resistant nonfamilial focal segmental glomerulosclerosis. *J Am Soc Nephrol* 2001; 12 (12): 2742–2746.
72. Kim JM, Wu H, Green G, Winkler CA, Kopp JB, Miner JH, Unanue ER, Shaw AS. CD2-associated protein haploinsufficiency is linked to glomerular disease susceptibility. *Science* 2003; 300 (5623): 1298–1300.
73. Mukerji N, Damodaran TV, Winn MP. TRPC6 and FSGS: the latest TRP channelopathy. *Biochim Biophys Acta* 2007; 1772 (8): 859–868.
74. Schell C, Huber TB. New players in the pathogenesis of focal segmental glomerulosclerosis. *Nephrol Dial Transplant*. 2012;27(9):3406-12.
75. Brown EJ, Schlöndorff JS, Becker DJ, Tsukaguchi H, Tonna SJ, Uscinski AL, Higgs HN, Henderson JM, Pollak MR. Mutations in the formin gene INF2 cause focal segmental glomerulosclerosis. *Nat Genet*. 2010;42(1):72-6.
76. Wei C, El Hindi S, Li J, Circulating urokinase receptor as a cause of focal segmental glomerulosclerosis. *Nat Med*. 2011; 17(8):952-960. 18.
77. McCarthy ET, Sharma M, Savin VJ. Circulating permeability factors in idiopathic nephrotic syndrome and focal segmental glomerulosclerosis. *Clin J Am Soc Nephrol*. 2010 Nov;5(11):2115-21. Review.
78. Audard V, Lang P, Sahali D Minimal change nephrotic syndrome: new insights into disease pathogenesis. *Med Sci (Paris)* 2008; 24 (10): 853–858.
79. Wernerson A, Dunér F, Pettersson E, Widholm SM, Berg U, Ruotsalainen V, Tryggvason K, Hulténby K, Söderberg M. Altered ultrastructural distribution of

- nephrin in minimal change nephrotic syndrome. *Nephrol Dial Transplant* 2003; 18: 70–76.
80. Ling C, Liu X, Shen Y, Chen Z, Fan J, Jiang Y, Meng Q. Urinary CD80 levels as a diagnostic biomarker of minimal change disease. *Pediatr Nephrol.* 2015;30(2):309-16.
 81. Yu CC, Fornoni A, Weins A, Hakrrouch S, Maiguel D, Sageshima J, Chen L, Ciancio G, Faridi MH, Behr D, Campbell KN, Chang JM, Chen HC, Oh J, Faul C, Arnaout MA, Fiorina P, Gupta V, Greka A, Burke GW 3rd, Mundel P. Abatacept in B7-1-positive proteinuric kidney disease. *N Engl J Med.* 2013;369(25):2416-23.
 82. Correspondence, *New England Journal* 2014, 370;13.
 83. Berger J, Hinglais N: Les dépôts intercapillaires d'IgA-IgG. *J Urol Nephrol* 1968; 74: 694–695.
 84. Yasuhiko Tomino. Immunopathological Predictors of Prognosis in IgA Nephropathy. Chen N (ed): *New Insights into Glomerulonephritis. Contrib Nephrol.* Basel, Karger, 2013, vol 181, pp 65–74.
 85. Yamaji K, Suzuki Y, Suzuki H, Satake K, Horikoshi S, Novak J, Tomino Y. The kinetics of glomerular deposition of nephritogenic IgA. *PLoS One.* 2014, 19;9(11):e113005.
 86. Lemley KV, Lafayette RA, Safai M, Derby G, Blouch K, Squarer A, Myers BD. Podocytopenia and disease severity in IgA nephropathy. *Kidney Int.* 2002;61(4):1475-85.
 87. Vogelmann SU, Nelson WJ, Myers BD, Lemley KV. Urinary excretion of viable podocytes in health and renal disease. *Am J Physiol Renal Physiol.* 2003;285(1):F40-8.
 88. Roberts IS. Oxford classification of immunoglobulin A nephropathy: an update. *Curr Opin Nephrol Hypertens.* 2013;22(3):281-6.
 89. Working Group of the International IgA Nephropathy Network and the Renal Pathology Society, Cattran DC, Coppo R, Cook HT, Feehally J, Roberts IS, Troyanov S, Alpers CE, Amore A, Barratt J, Berthoux F, Bonsib S, Bruijn JA, D'Agati V, D'Amico G, Emancipator S, Emma F, Ferrario F, Fervenza FC, Florquin S, Fogo A, Geddes CC, Groene HJ, Haas M, Herzenberg AM, Hill PA, Hogg RJ, Hsu SI, Jennette JC, Joh K, Julian BA, Kawamura T, Lai FM, Leung CB, Li LS, Li PK, Liu ZH, Mackinnon B, Mezzano S, Schena FP, Tomino Y, Walker PD, Wang H, Weening JJ, Yoshikawa N, Zhang H. The Oxford classification of IgA nephropathy: rationale, clinicopathological correlations, and classification. *Kidney Int.* 2009;76(5):534-45.
 90. Working Group of the International IgA Nephropathy Network and the Renal Pathology Society, Roberts IS, Cook HT, Troyanov S, Alpers CE, Amore A, Barratt J, Berthoux F, Bonsib S, Bruijn JA, Cattran DC, Coppo R, D'Agati V,

D'Amico G, Emancipator S, Emma F, Feehally J, Ferrario F, Fervenza FC, Florquin S, Fogo A, Geddes CC, Groene HJ, Haas M, Herzenberg AM, Hill PA, Hogg RJ, Hsu SI, Jennette JC, Joh K, Julian BA, Kawamura T, Lai FM, Li LS, Li PK, Liu ZH, Mackinnon B, Mezzano S, Schena FP, Tomino Y, Walker PD, Wang H, Weening JJ, Yoshikawa N, Zhang H.
The Oxford classification of IgA nephropathy: pathology definitions, correlations, and reproducibility. *Kidney Int.* 2009;76(5):546-56.

91. Katafuchi R, Ninomiya T, Nagata M, et al. Validation study of Oxford Classification of IgA nephropathy: the significance of extracapillary proliferation. *Clin J Am Soc Nephrol* 2011; 6:2806–2813.
92. Zeng CH, Le W, Ni Z et al. A multicenter application and evaluation of the oxford classification of IgA nephropathy in adult chinese patients. *Am J Kidney Dis* 2012; 60: 812–820.
93. Shi SF, Wang SX, Jiang L et al. Pathologic predictors of renal outcome and therapeutic efficacy in IgA nephropathy: validation of the oxford classification. *Clin J Am Soc Nephrol* 2011; 6: 2175–2184.
94. Yau T, Korbet SM, Schwartz MM et al. The Oxford classification of IgA nephropathy: a retrospective analysis. *Am J Nephrol* 2011; 34: 435–444.
95. Yang YH, Yu HH, Chiang BL. The diagnosis and classification of Henoch-Schönlein purpura: an updated review. *Autoimmun Rev.* 2014;13(4-5):355-8.
96. Lai WL, Yeh TH, Chen PM, Chan CK, Chiang WC, Chen YM, Wu KD, Tsai TJ. Membranous nephropathy: A review on the pathogenesis, diagnosis, and treatment. *J Formos Med Assoc.* 2015 Jan 2. pii: S0929-6646(14)00295-2.
97. Nangaku M, Shankland SJ, Couser WG. Cellular response to injury in membranous nephropathy. *J Am Soc Nephrol.* 2005;16(5):1195-204.
98. Beck LH Jr, Bonegio RG, Lambeau G, Beck DM, Powell DW, Cummins TD, Klein JB, Salant DJ. M-type phospholipase A2 receptor as target antigen in idiopathic membranous nephropathy. *N Engl J Med* 2009;361:11e21.
99. Stanescu HC, Arcos-Burgos M, Medlar A, Bockenhauer D, Kottgen A, Dragomirescu L, et al. Risk HLA-DQA1 and PLA(2)R1 alleles in idiopathic membranous nephropathy. *N Engl J Med* 2011;364:616e26.
100. Prunotto M, Carnevali ML, Candiano G, Murtas C, Bruschi M, Corradini E, et al. Autoimmunity in membranous nephropathy targets aldose reductase and SOD2. *J Am Soc Nephrol* 2010; 21:507e19. 46.
101. Murtas C, Bruschi M, Candiano G, Moroni G, Magistroni R, Magnano A, et al. Coexistence of different circulating antipodocyte antibodies in membranous nephropathy. *Clin J Am Soc Nephrol* 2012;7:1394e400.
102. Tomas NM, Beck LH Jr, Meyer-Schwesinger C, Seitz-Polski B, Ma H, Zahner G, Dolla G, Hoxha E, Helmchen U, Dabert-Gay AS, Debayle D, Merchant M, Klein J, Salant DJ, Stahl RA, Lambeau G Thrombospondin type-

- 1 domain-containing 7A in idiopathic membranous nephropathy. *N Engl J Med.* 2014 Dec 11;371(24):2277-87.
103. Simic I, Tabatabaeifar M, Schaefer F. Animal models of nephrotic syndrome. *Pediatr Nephrol.* 2013;28(11):2079-88.
104. Suzuki H, Suzuki Y, Novak J, Tomino Y. Development of Animal Models of Human IgA Nephropathy. *Drug Discov Today Dis Models.* 2014 ;11:5-11.
105. Mimura I, Kanki Y, Kodama T, Nangaku M. Revolution of nephrology research by deep sequencing: ChIP-seq and RNA-seq. *Kidney Int.* 2014;85(1):31-8.
106. Renkema KY, Stokman MF, Giles RH, Knoers NV. Next-generation sequencing for research and diagnostics in kidney disease. *Nat Rev Nephrol.* 2014;10(8):433-44.
107. Bamshad, M. J. et al. Exome sequencing as a tool for Mendelian disease gene discovery. *Nat. Rev. Genet.* 2011;12, 745–755.
108. Wang Y, Wang YP, Tay YC, Harris DC. Progressive adriamycin nephropathy in mice: sequence of histologic and immunohistochemical events. *Kidney Int.* 2000;58(4):1797-804.
109. Ryan G KMJ: An ultrastructural study of the mechanisms of proteinuria in aminonucleoside nephrosis. *Kidney Int* 1975;8:219–232.
110. Dunér F, Lindström K, Hultenby K, Hulkko J, Patrakka J, Tryggvason K, Haraldsson B, Wernerson A, Pettersson E. Permeability, ultrastructural changes, and distribution of novel proteins in the glomerular barrier in early puromycin aminonucleoside nephrosis. *Nephron Exp. Nephrol.* 2010;116(2):e42-52.
111. Sun Y, He L, Takemoto M et al. Glomerular transcriptome changes associated with lipopolysaccharide-induced proteinuria, (+ supplementary material). *Am J Nephrol* 2009; 29: 558–570.
112. Weibel, E. Stereological methods: practical methods for biological morphometry, vol. 1. Academic: London, 1979.
113. Sekar RB, Periasamy A. Fluorescence resonance energy transfer (FRET) microscopy imaging of live cell protein localizations. *J Cell Biol.* 2003;160(5):629-33. Review.
114. de Mik SM, Hoogduijn MJ, de Bruin RW, Dor FJ. Pathophysiology and treatment of focal segmental glomerulosclerosis: the role of animal models. *BMC Nephrol.* 2013;14:74.
115. Asanuma K, Akiba-Takagi M, Kodama F, Asao R, Nagai Y, Lydia A, Fukuda H, Tanaka E, Shibata T, Takahara H, Hidaka T, Asanuma E, Kominami E, Ueno T, Tomino Y. Dendrin location in podocytes is associated

- with disease progression in animal and human glomerulopathy. *Am J Nephrol*. 2011;33(6):537-49.
116. Kodama F, Asanuma K, Takagi M, Hidaka T, Asanuma E, Fukuda H, Seki T, Takeda Y, Hosoe-Nagai Y, Asao R, Horikoshi S, Tomino Y. Translocation of Dendrin to the podocyte nucleus in acute glomerular injury in patients with IgA nephropathy. *Nephrol Dial Transplant*. 2013 (7):1762-72.
 117. Greene CN, Keong LM, Cordovado SK *et al*. Sequence variants in the PLEKHH2 region are associated with diabetic nephropathy in the GoKinD study population. *Hum Genet* 2008; 124 (3): 255–262.
 118. Takahashi A, Fukusumi Y, Yamazaki M, Kayaba M, Kitazawa Y, Tomita M, Kawachi H. Angiotensin II type 1 receptor blockade ameliorates proteinuria in puromycin aminonucleoside nephropathy by inhibiting the reduction of NEPH1 and nephrin. *J Nephrol*. 2014, [Epub ahead of print]
 119. Maija Suvanto, Timo Jahnukainen, Marjo Kestila, Hannu Jalanko. Podocyte proteins in congenital and minimal change nephrotic Syndrome. *Clin Exp Nephrol* 2014; [Epub ahead of print].
 120. Patrakka J, Ruotsalainen V, Ketola I, Holmberg C, Heikinheimo M, Tryggvason K, Jalanko H. Expression of nephrin in pediatric kidney diseases. *J Am Soc Nephrol* 2001; 12 (2): 289–296.
 121. Koop K, Eikmans M, Baelde HJ, Kawachi H, De Heer E, Paul LC, Bruijn JA. Expression of podocyte-associated molecules in acquired human kidney diseases. *J Am Soc Nephrol* 2003; 14 (8): 2063–2071.
 122. Kim BK, Hong HK, Kim JH, Lee HS. Differential expression of nephrin in acquired human proteinuric diseases. *Am J Kidney Dis* 2002; 40 (5): 964–973.
 123. Doublier S, Ruotsalainen V, Salvidio G, Lupia E, Biancone L, Conaldi PG, Reponen P, Tryggvason K, Camussi G. Nephrin redistribution on podocytes is a potential mechanism for proteinuria in patients with primary acquired nephrotic syndrome. *Am J Pathol* 2001; 158: 1723–1731.
 124. Lasagni L, Lazzeri E, Shankland SJ, Anders HJ, Romagnani P. Podocyte mitosis - a catastrophe. *Curr Mol Med*. 2013;13(1):13-23.
 125. Greka A, Mundel P. Cell biology and pathology of podocytes. *Annu Rev Physiol* 2012; 74: 299-323.
 126. Sciffer M, Shaw AS, Mundel P, A novel role for the adaptor molecule CD-associated protein in transforming growth factor-beta-induced apoptosis. *J Biol Chem* 2004;279:37004-37012.
 127. Verma R, Kovari I, Soofi A, Nihalani D, Patrie K, Holzman LB. Nephrin ectodomain engagement results in Src kinase activation, nephrin phosphorylation, Nck recruitment, and actin polymerization.

J Clin Invest. 2006;116(5):1346-59.

128. Wagner MC¹, Rhodes G, Wang E, Pruthi V, Arif E, Saleem MA, Wean SE, Garg P, Verma R, Holzman LB, Gattone V, Molitoris BA, Nihalani D. Ischemic injury to kidney induces glomerular podocyte effacement and dissociation of slit diaphragm proteins Neph1 and ZO-1. J Biol Chem. 2008;283(51):35579-89.
129. Harita Y, Kurihara H, Kosako H, Tezuka T, Sekine T, Igarashi T, Hattori S. Neph1, a component of the kidney slit diaphragm, is tyrosine-phosphorylated by the Src family tyrosine kinase and modulates intracellular signaling by binding to Grb2. J Biol Chem. 2008; 4;283(14):9177-86.
130. Kerjaschki D. Polycation-induced dislocation of slit diaphragms and formation of cell junctions in rat kidney glomeruli: the effects of low temperature, divalent cations, colchicine, and cytochalasin B. Lab Invest. 1978;39(5):430-40.
131. Garg P, Verma R, Cook L, Soofi A, Venkatareddy M, George B, Mizuno K, Gurniak C, Witke W, Holzman LB. Actin-depolymerizing factor cofilin-1 is necessary in maintaining mature podocyte architecture. J Biol Chem. 2010;16;285(29):22676-88.
132. Arif E, Rathore YS, Kumari B, Ashish F, Wong HN, Holzman LB, Nihalani D. Slit diaphragm protein Neph1 and its signaling: a novel therapeutic target for protection of podocytes against glomerular injury. J Biol Chem. 2014 4;289(14):9502-18
133. Xiao Z, Rodriguez PQ, He L, Betsholtz C, Tryggvason K, Patrakka J. Wtip- and gadd45a-interacting protein dendrin is not crucial for the development or maintenance of the glomerular filtration barrier. PLoS One. 2013 20;8(12):e83133.